

**HYDRODEOXYGENATION OF LIGNIN MODEL COMPOUNDS
VIA THERMAL CATALYTIC REACTIONS**

A M.S. Thesis
Presented to
The Academic Faculty

by

Michael Joseph Roy

In Partial Fulfillment
of the Requirements for the Degree
Master of Science in the
School of Chemical and Biomolecular Engineering

Georgia Institute of Technology
December 2012

HYDRODEOXYGENATION OF LIGNIN MODEL COMPOUNDS VIA THERMAL CATALYTIC REACTIONS

Approved by:

Dr. Yulin Deng, Advisor
School of Chemical & Biomolecular Engineering
Georgia Institute of Technology

Dr. Sujit Banerjee
School of Chemical & Biomolecular Engineering
Georgia Institute of Technology

Dr. Jeffery Hsieh
School of Chemical & Biomolecular Engineering
Georgia Institute of Technology

Date Approved: July 18, 2012

To my parents and grandparents,
Thank you and I love you all.

Boooooooooo!

ACKNOWLEDGEMENTS

I wish to thank The Honorable Reverend Doctor Major Henry Hank White Williams Junior P. The Third, our grandfatherly head of security for the Institute of Paper Science and Technology, for keeping myself and others safe and laughing. I would also like to thank my good friends, Wei Mu and Sudhir Sharma, for their help when I had questions about my research. I would also like to thank Dr. Yulin Deng for supporting me over the last two years and guiding me during the process of earning my Master of Science Degree.

TABLE OF CONTENTS

	Page
ACKNOWLEDGEMENTS	iv
LIST OF TABLES	vii
LIST OF FIGURES	viii
LIST OF REACTION SCHEMES	x
SUMMARY	xi
<u>CHAPTER</u>	
1 Introduction	1
Background	3
Biomass	3
The Kraft Process	6
Turning Lignin into a Fuel	8
Review of the Literature	12
Methods of Converting Biomass	12
Liquefaction	12
Pyrolysis	13
Products Obtained from Thermochemical Biomass Routes	14
Liquefaction Products	14
Pyrolysis Products	15
Types of Upgrading	17
Physical Methods	17
Hydrodeoxygenation	18
Zeolite Cracking	18

Hydrodeoxygenation Catalyst Review	19
Hydrodeoxygenation Support Review	22
Hydrodeoxygenation Solvents Review	24
Literature Review Summary	27
Hydrogen Solubility	27
2 Hypothesis & Objectives	28
Hypothesis for Catalytic Hydrodeoxygenation (HDO) Reaction	28
Objectives	28
3 Experimental	29
Analysis Methods	29
UV-Vis	29
GC-MS	30
Materials and Reaction Conditions	31
Results	32
4 Summary	40
Conclusion	40
Recommendations for Future Work	40
REFERENCES	42

LIST OF TABLES

	Page
Table 1: Zeolites used for catalytic cracking of pyrolysis oil or model compounds and reaction temperature.	19
Table 2: Hydrodeoxygenation (HDO) catalysts, supports, and years of publication.	20
Table 3: Bond dissociation energies (kJ/mol).	24
Table 4: Catalysts, supports, model compounds, and solvents used in some hydrodeoxygenation reactions.	25

LIST OF FIGURES

	Page
Figure 1: Annual consumption and importation of biofuels in the U.S. since 1981. ¹	2
Figure 2: Lignocellulose composition: cellulose, hemicellulose, and lignin. ¹²	3
Figure 3: Crystalline cellulose	4
Figure 4: Representation of a softwood lignin structure. ⁹	5
Figure 5: Representation of a hardwood lignin structure. ⁹	6
Figure 6: Schematic representation of the Kraft cycle following the chemicals.	8
Figure 7: Common linkages found in lignin. ¹⁶	10
Figure 8: Van Krevelen diagram. ²⁰	11
Figure 9: Process schematic for biomass liquefaction, purification, and upgrading. ¹²	12
Figure 10: Bubbling fluid bed reactor with electrostatic precipitator. ²⁶	14
Figure 11: Yield of products during liquefaction of some biomass samples. ²⁸	15
Figure 12: Flow sheet for production of bio-fuels through pyrolysis and catalytic upgrading. ²⁷	17
Figure 13: Selectivity vs. phenol conversion for Pt/HY zeolite at 473 K; H ₂ pressure, 4 MPa; WHSV, 5-20 h ⁻¹ ; 2 h reaction time. ⁴³	22
Figure 14: Dibenzofuran (DBF) deoxygenation degree at varying LHSV. ³³	23
Figure 15: Gas, Liquid, and solid yields from treatment of model bio-oil with Pt catalysts. (Reaction time of 2 h with initial mass of synthetic bio-oil = 40 g) ⁴⁶	26
Figure 16: Oxygen content of oil product obtained from treatment of synthetic bio-oil with Pt/Al ₂ O ₃ . ⁴⁶	26
Figure 17: UV-Vis of three standard guaiacol solutions in water.	30
Figure 18: Comparison of guaiacol conversion at 250 psig, 3 hr reaction time at varying temperature for heptane and water solvents.	33
Figure 19: Comparison of guaiacol conversion by UV-Vis at 500 psig, 3 hr reaction time at varying temperature for heptane and water solvents.	33

Figure 20: Guaiacol conversion at varying temperature and pressure in heptane solvent at 3 h by UV-Vis.	34
Figure 21: Guaiacol conversion at varying temperature and pressure in aqueous solvent at 3 h by UV-Vis.	34
Figure 22: Comparison of solvents with time at 250 psig and 250°C by UV-Vis.	35
Figure 23: Analytical measurement comparison for heptane solvent at 250 psig and 3 h.	36
Figure 24: Analytical measurement comparison for heptane solvent at 500 psig and 3 h.	36
Figure 25: Conversion comparison of analytical measurements for water solvent at 500 psig and 3 h.	37
Figure 26: Hydrodeoxygenation products observed from the GC-MS.	37
Figure 27: Products from guaiacol, identified by GC-MS, in heptane at 250 psig for 3 hours.	38
Figure 28: Products from guaiacol, identified by GC-MS, in heptane at 500 psig for 3 hours.	38
Figure 29: Reaction products via GC-MS at 250 psig H ₂ and 250°C in heptane for various times.	39

LIST OF REACTION SCHEMES

	Page
Scheme 1: Reaction pathway of phenol with Pt/HY zeolite catalyst. ⁴³	22
Scheme 2: Schematic expression of the DBF reaction pathway. ³³	23
Scheme 3: Proposed reaction pathway for the hydrodeoxygenation of guaiacol with Pt/C catalyst.	32

SUMMARY

Lignin is an important component of biomass accounting for up to 30% by weight but up to 40% of the total energy content of the plant. As the push towards alternative fuels develops, more and more amounts of lignin will be gathered and used predominately as low grade boiler fuel to run primary processes. We argue there is usefulness in the conversion of lignin into value added specialty chemicals and fuels. In this work, a new approach for hydrodeoxygenation of lignin model compounds using platinum as the catalyst and organic solvent as the reaction medium was conducted, and the results were compared with those obtained using water as the reaction medium. It is shown that the organic solvent is able to hydrogenate the model compound with the same effect at lower temperature, hydrogen pressure, and time.

CHAPTER 1

INTRODUCTION

Domestic energy consumption is continuing to expand and further resources will need to be tapped in the future to accommodate growth and expansion while reducing the exploitation of dead dinosaur fuel. There are many highlights in the United States alone for the consumption of energy including:^{1,2}

- Domestic energy consumption has increased by 28% since 1973 from 75 to 97 quadrillion Btu of energy with a large percentage (28% in 2010) of energy used for the transportation sector.
- Annual energy consumption from renewable resources is on pace to double from the year 2001 to 2012.
- Renewable energies now contribute more energy to domestic consumption than that of nuclear electric power.
- Annual consumption of fuel ethanol has more than tripled between 2005 and 2011 while biodiesel is on pace to more than double in 2012 over the previous year.

The remarkable growth in renewable transportation fuels in the U.S. is being realized due to changes in economic and political policies as well as changing consumer demand. Changes in U.S. ethanol and biodiesel consumption over the years can be seen in figure 1 below. Politicians are quick to throw out buzz phrases and tout national security concerns for the impetus to increase alternative fuels production, even though we import 33% less petroleum from OPEC countries than non-OPEC countries.¹ Environmentalists and scientists make the argument to reduce carbon emissions which

have been shown to contribute to global warming and cause changes to farming practices³⁻⁸.

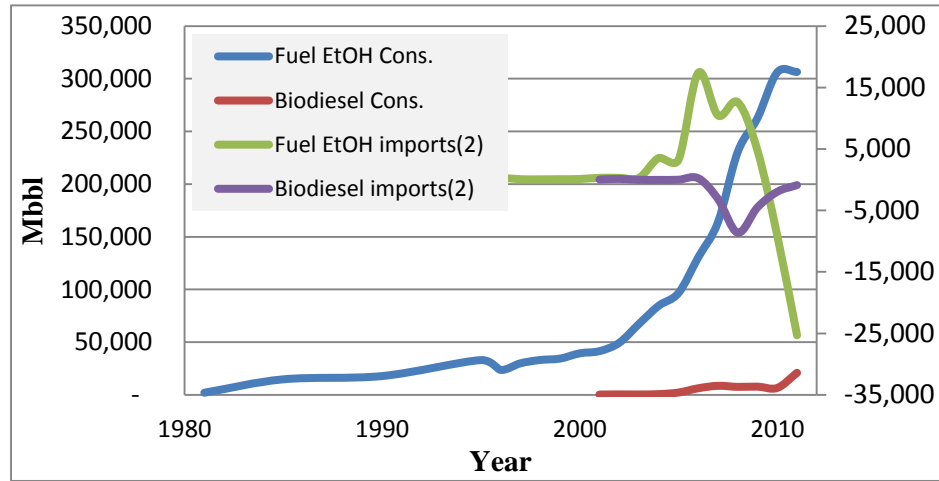


Figure 1. Annual consumption and importation of biofuels in the U.S. since 1981.¹ (2) signifies secondary axis.

There is a vast potential supply of sustainable renewable biomass from forest and agricultural lands throughout the world. The United States alone has the ability to provide more than 1.3 billion dry tons annually to supply biorefineries.⁹ Therefore, it is imperative that efforts are contributed towards advancing the science of converting renewable materials such as trees into other useful products such as fuels, specialty chemicals, and plastics. Parikka claimed the sustainable global biomass energy potential is $\sim 10^{20}$ J per year ($\sim 9.478 \times 10^{16}$ Btu per year) and $\sim 40\%$ was being used.¹⁰ It is also imperative that all fractions of the tree be used for the highest value products obtainable for that specific fraction. There has been a great deal of research with turning cellulose and hemicellulose into ethanol, while lignin has been utilized predominately as an agricultural waste for the production of steam to run the process. However, lignins' unique structure is well suited for specialty chemicals and high value fuels.

Background

Biomass

Plants are comprised of mainly three polymers accounting for more than 90% of the total weight on a dry mass basis. Lignocellulosic biomass consists of cellulose: 35-50%, hemicellulose: 25-30%, and lignin: 15-30% by weight. Lignin may contribute up to 40% of the total energy content of the plant.^{9,11,12} A figure of the plants constituents from work by Dumesic is shown below. Certain differences in the content of biomass fractions between grasses, softwoods and hardwoods are known and can be estimated. Softwoods tend to have a higher percentage of lignin with a lesser percentage of hemicellulose when compared to hardwoods.

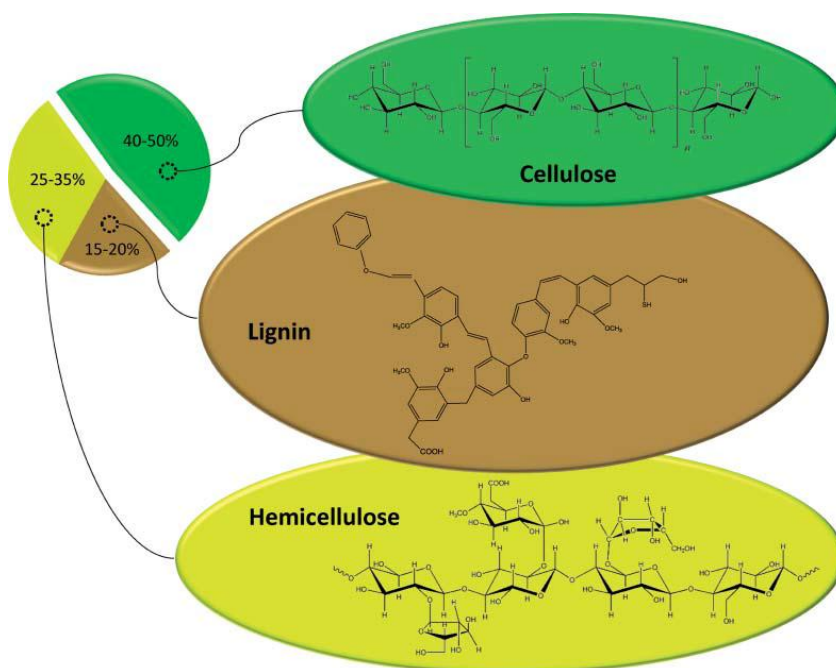


Figure 2. Lignocellulose composition: cellulose, hemicellulose, and lignin.¹²

Cellulose is a biopolymer consisting of β -(1,4)-glucan with a high degree of polymerization between 300 and 15,000 base units.¹¹ Cellulose is principally a crystalline polymer due to complimenting hydrogen bonding between adjacent hydrogens and

oxygens aside the main chain. Amorphous cellulose can behave quite differently from crystalline and one example is the preferential destruction of amorphous cellulose over crystalline cellulose by cellulase. Cellulose is not branched so alignment of the hydrogen bonding tends to make the hydrogen bonding very secure and difficult to fractionate.

Figure 3 depicts the crystalline structure of cellulose.

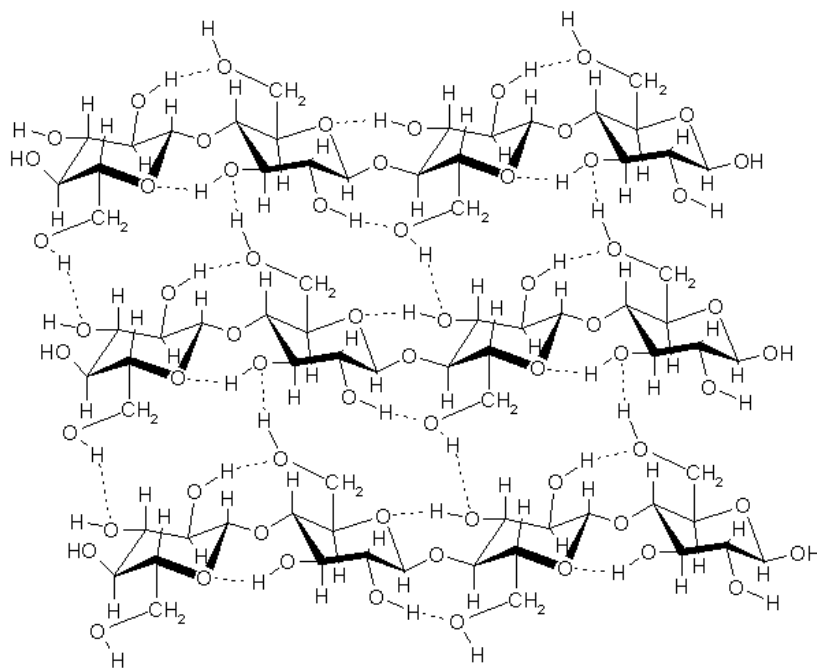


Figure 3. Crystalline cellulose.

Cellulose can be broken apart with cellulase and ultimately converted into ethanol by common baker's yeast (*Saccharomyces cerevisiae*) somewhat similar to the production of beer, wine, and other spirits. Other advances in transforming the hemicellulose fraction have targeted metabolic engineering of microorganisms such as *Zymomonas mobilis* and *Escherichia coli* with good success.¹³

Hemicellulose is a branched and substituted polysaccharide of various sugars such as glucan, mannan, and xylans. The degree of polymerization is lower than that of cellulose at 70-200 base units.¹¹ Hemicellulose is used by the plant to improve structural properties by providing bonding between cellulose "rods" through hydrogen bonding and direct linkages. Hemicellulose is bound with lignin and cellulose can be interwoven into

and between hemicellulose portions of the plant. Once isolated, the xylose monomers are very suitable feedstocks for ethanol production via fermentation or dehydrated to furfural.¹²

Lignin is a highly branched three-dimensional amorphous polymer consisting of varying degrees of methoxylated phenylpropane structures, such as coniferyl alcohol, sinapyl alcohol, and coumaryl alcohol.^{9,14,15} Lignin provides protection and support for the tree by: increasing hydrophobicity to keep water and bacteria or viruses out, improving thermoplasticity, allowing for dimensional changes within the cell wall during changes in moisture, and increasing structural support for the cell walls. Grasses, hardwoods and softwoods show differences in the amounts of each monolignol present in the structure of lignin. Grasses consist primarily of p-coumaryl alcohol, coniferyl alcohol tends to dominate softwoods, and there is about an equal amount of coniferyl and sinapyl alcohols in hardwoods.¹⁶ A representation of soft and hardwood lignins is shown in figures 4 and 5, but does not necessarily depict the native lignin structure.^{9,17}

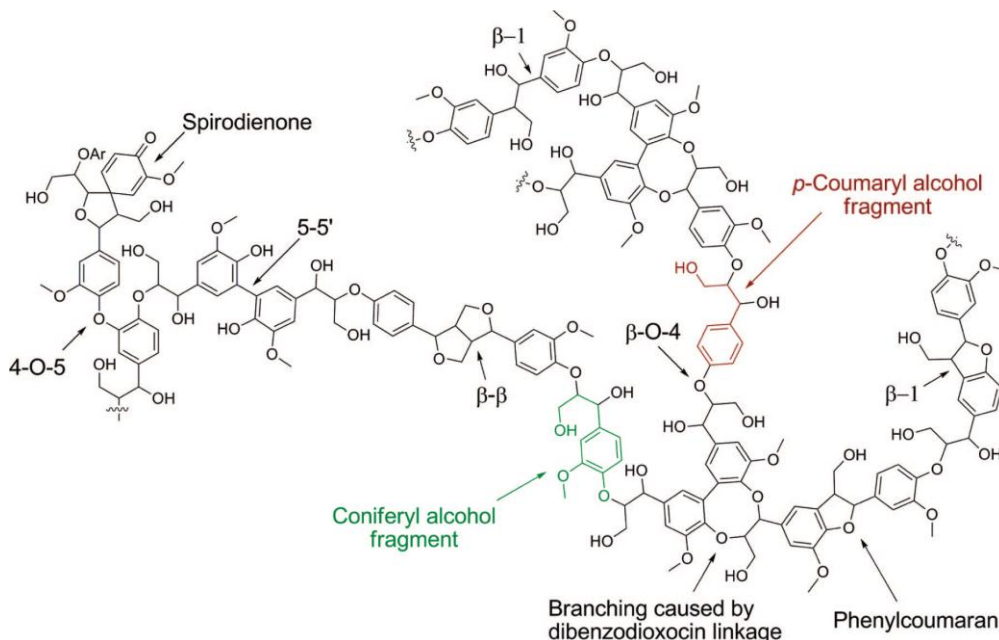
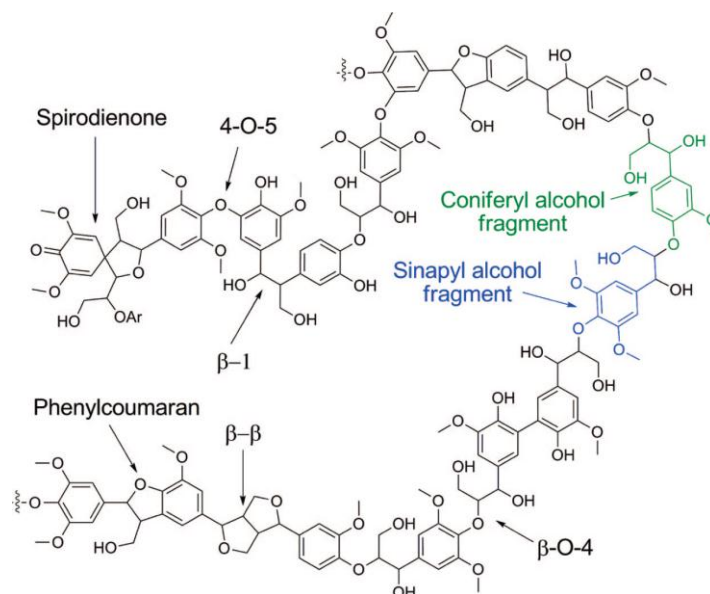


Figure 4. Representation of a softwood lignin structure.⁹



Figures 5. Representation of a hardwood lignin structure.⁹

There is a vast supply of isolated lignin, predominantly from the Kraft process in the pulp and paper industry. In 2004, the pulp and paper industries produced 50 million tons of extracted lignin, but only 2% is used commercially for products like dispersing or binding agents with the remainder burned as a low value fuel. The average monomeric chemical formula for softwood kraft lignin is ${}^9\text{C}_9\text{H}_{8.5}\text{O}_{2.1}\text{S}_{0.1}(\text{OCH}_3)_{0.8}(\text{CO}_2\text{H})_{0.2}$, showing a substantially lower O/C ratio than cellulose's 1.

The Kraft process

Debarked, typically softwood, trees are chipped into an ideally uniform thickness of ~2mm and cooked in a pressurized cylinder filled with ~20% NaOH, ~5% NaSH, and four times as much water by weight than chips. The vessel is closed and the reactor is heated to 443 K for about two hours while continuously recirculating the liquid contents. The lignin is degraded and becomes soluble along with a large portion of the hemicellulose and extractives contained in the wood. The vessel is opened and the original structure of the chips is easily broken apart during the blow. The mixture of cellulose fibers and liquid is filtered through continuous rotary drum filters where the

fibers are recovered and used for making paper products. The filtrate contains much water, lignin, and pulping chemicals which must be recovered to keep the plant running economically. Water is evaporated in the multiple effect evaporators to increase the heating value of the black liquor. The evaporators and steam injectors decrease the percent water from 85 down to about 20. The heating value of the heavy black liquor feeding the recovery boiler is 8-10 MJ/kg. Steam is generated at the boiler from the combustion of lignin and the pulping chemicals fall to the bottom where they are removed from the boiler, mixed with water becoming green liquor. The steam generated is used in the multiple effect evaporators and in other heating applications throughout the mill. The green liquor is recausticized and converted back into useful pulping chemicals for new cooks in the digester. Good operations are able to recover all but 1% of the chemicals necessary for a complete cycle. A schematic of the Kraft process is shown in figure 6.

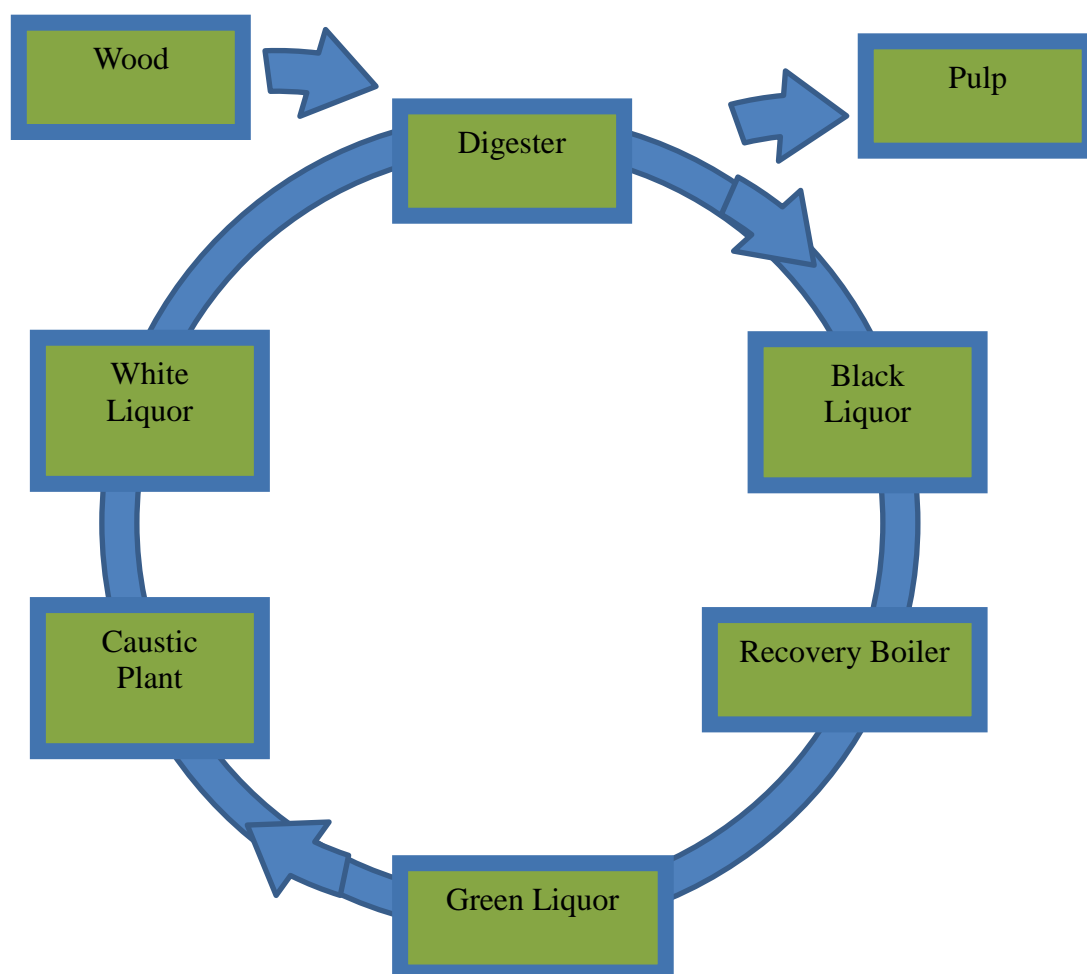


Figure 6. Schematic representation of the Kraft cycle following the chemicals.

Turning Lignin into a Fuel

Lignin is a large biopolymer with a high molecular weight in the thousands. When extracted, it is typically an insoluble solid and therefore not capable of being used in traditional automobile engines. Fortunately, the base quantity of ~10 carbons in lignin is similar to that of gasoline and diesel type fuels.⁹ Gasoline is a blend of ~C5 to C10 hydrocarbons (MW of 72-142) while diesel fuel typically relies on C12 to C20 hydrocarbons (MW of 170-282).¹¹ In order to transform the solid and high molecular weight polymer into monomeric products more suitable as a liquid fuel involves the cleavage of its interunit linkages.

Fortunately, the number of linkages between monolignols is limited and dominated by only a few types. The β -O-4 type accounts for about half of all bonds, the 5-5' biphenyl bond contributes up to 25%, and the phenylcoumaran and diphenyl ethane each at about 10%.^{14,16} Depictions of the common linkages can be seen below in figure 7. There are a number of methods used to dissociate lignin into smaller fractions such as enzymes, pyrolysis, gasification, ionic liquids, hydrogenolysis, oxidation, and simply combustion. Each process has its advantages and disadvantages in terms of costs to construct, operate, energy inputs, and the products needed. Enzymatic degradation may take a long amount of time, but would preserve the original structure of native lignin more so than perhaps other types of chemical and energy intensive processes.¹⁸ Gasification would yield large amount of carbon monoxide, hydrogen, carbon dioxide and tars. Pyrolysis uses a milder temperature (up to $\sim 700^{\circ}\text{C}$) than gasification in the absence of oxygen to crack weaker bonds forming simpler compounds resembling lignin in the monomer to trimer range.¹⁹ Hydrogenolysis is performed at elevated temperature in solution with hydrogen to cleave bonds. The hydrogen source can be dissolved in solution or be actively donated by the solution itself such as tetralin, sodium formate, or formic acid.¹⁸ Hydrogen donating solvent pose an interesting route by having hydrogen generated in the immediate vicinity of the catalyst and by diluting the sample which helps in reducing occurrence of polymerization reaction. We briefly investigated the use of formic acid and found the temperature required for hydrogen generation to be near the temperature limit of our reactor. If generation of hydrogen could occur at lower temperatures, this would be a most interesting route to use.

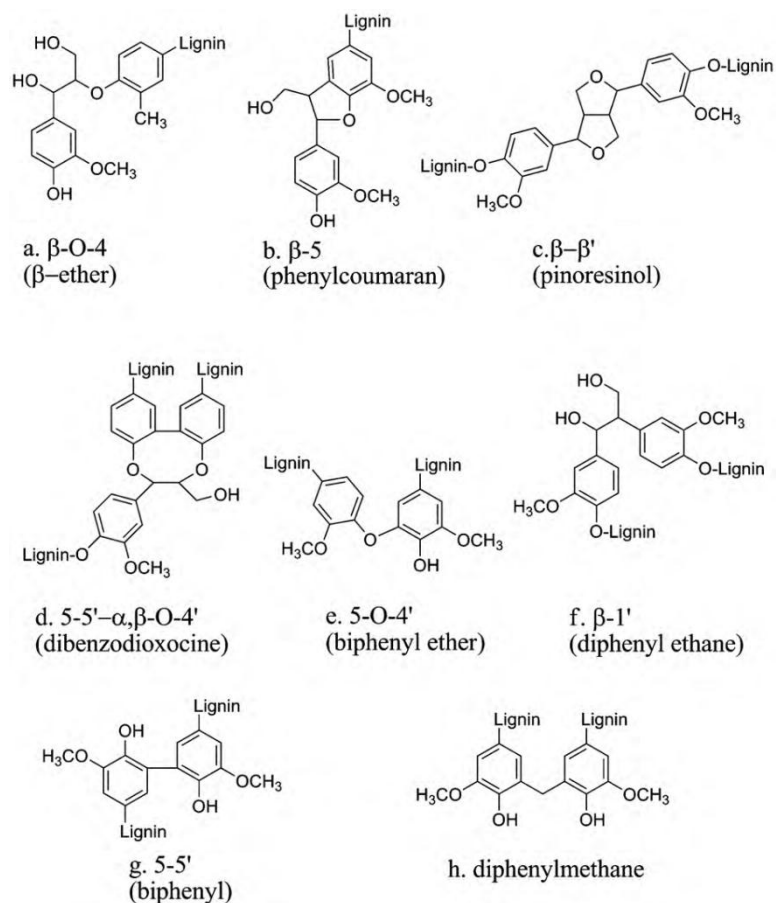


Figure 7. Common linkages found in lignin.¹⁶

Regardless of the source of reduced molecular weight products, most will have a fairly large proportion of oxygen to carbon thereby reducing the calorific value. The Van Krevelen diagram below shows various types of fuels according to their hydrogen and oxygen to carbon ratios. Using DuLong's formula, it can be shown that the highest calorific value of a fuel is related to the H/C ratio and more importantly the O/C ratio.

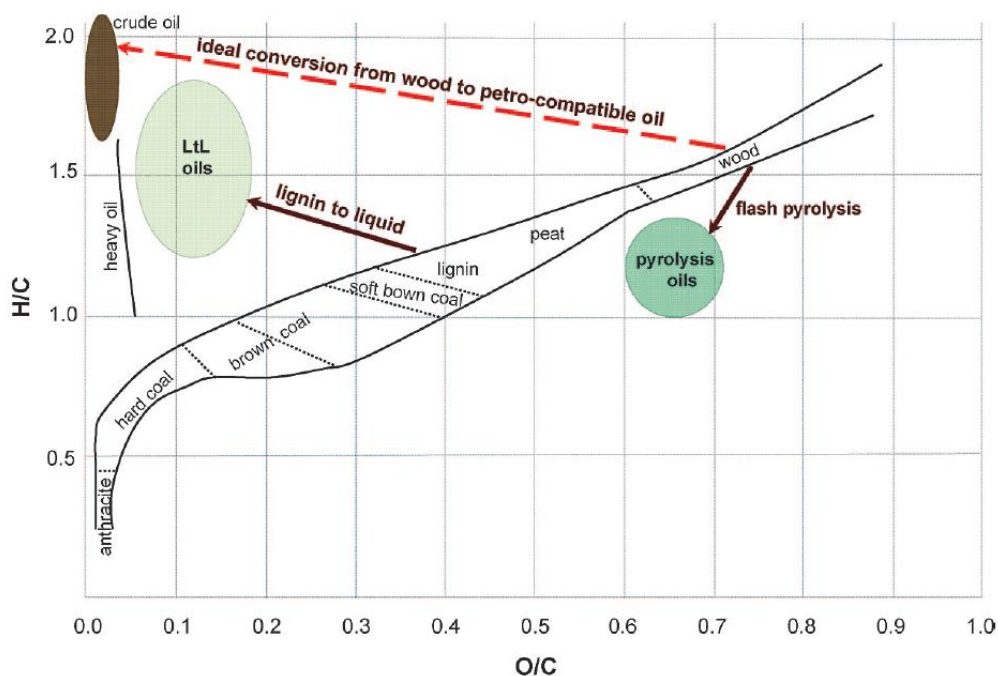


Figure 8. Van Krevelen diagram.²⁰

Dulong's formula²¹ is shown below based on a percent mass basis excluding sulfur. It can be seen that carbons and hydrogens add to the calorific value while oxygen, pi bonds, and rings would reduce the energy density of the fuel. Therefore, the highest energy density would be on the upper left of the Van Krevelen diagram shown above.

$$HHV (MJ/kg) = 0.3382 * \%C + 1.4428(\%H - (\%O)/8)$$

Reduction in the relative content of oxygen of lignin derived monomers will have the greatest impact into its usefulness as a liquid fuel.

Review of the Literature

Methods of Converting Biomass

There are many processes to convert biomass into useful forms of energy or specialty chemicals including gasification, pyrolysis, liquefaction, catalytic processes, and biochemical processes.¹² Of the thermochemical routes for upgrading biomass to liquid fuels, pyrolysis and liquefaction both produce what is generally referred to as bio-oil. The thermochemical routes are more general processes applicable to a wider variety of biomasses than the hydrolysis pathways.

Liquefaction

Liquefaction processes involve grinding the biomass to between 0.5 and 50mm (desire 10-15mm) that is mixed with water or recycled wood-derived oil with basic catalysts such as sodium carbonate or potassium carbonate and pressurized to 5-250 atm with hydrogen or syngas. Typical process temperature ranges from 525-725 K with residence times of 4-30 minutes.^{12,22,23,24} Figure 9 shows the process schematic for biomass liquefaction.

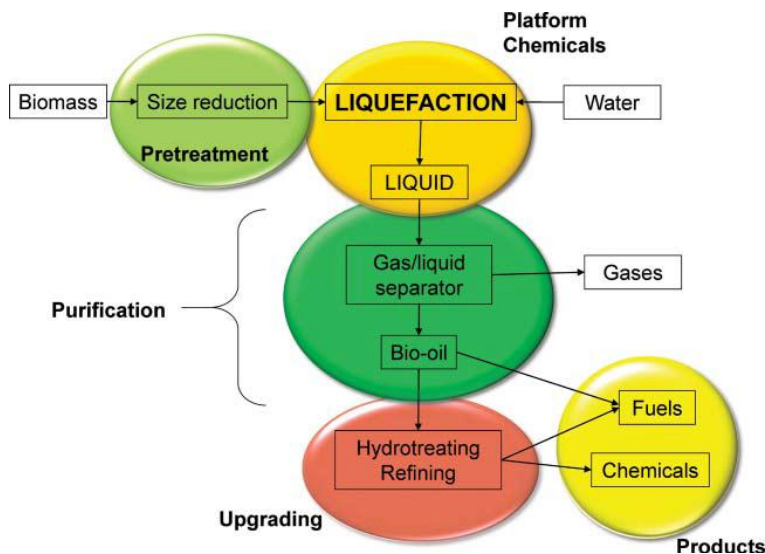


Figure 9. Process schematic for biomass liquefaction, purification, and upgrading.¹²

Pyrolysis

Pyrolysis is the anaerobic decomposition of biomass at elevated temperatures of 573 to 873 K in vacuum to several atmospheres of pressure. The biomass must be size reduced to a larger degree than that found in liquefaction processes to ensure rapid and uniform heating on the order of 10^3 - 10^4 K s⁻¹. There are several types of pyrolysis depending on the reaction time of minutes (slow) to as little as one second (fast or flash pyrolysis). In general, the longer the vapors are at elevated temperature, greater amounts of char can be formed with fewer oil products. Therefore, fast pyrolysis is considered the path forward in terms of the route of pyrolysis. Fast pyrolysis yields of bio-oil can be 60-75 wt.% composed of more than 350 compounds including aromatics, acids, aldehydes, alcohols, sugars, esters, and ketones. Solid char accounts for 15-25 wt.% while 10-20 wt.% of noncondensable gases are formed from fast pyrolysis depending on the feedstock.²⁵ Pyrolysis can be performed on a variety of different biomass and will even transform difficult to manage components such as lignin.

Figure 10 shows the process outline for a bubbling fluidized bed pyrolysis reactor. The dried and size reduced biomass is inserted via a plugged screw conveyor to the reactor where hot gases are in contact with the biomass which is first dried completely and then volatilized. The remaining biomass (char) is separated and used for heat generation. The product gases are subsequently cooled to condense the bio-oil. Bio-oil is highly reactive and will readily polymerize when exposed to temperatures near 373 K.^{12,26,27}

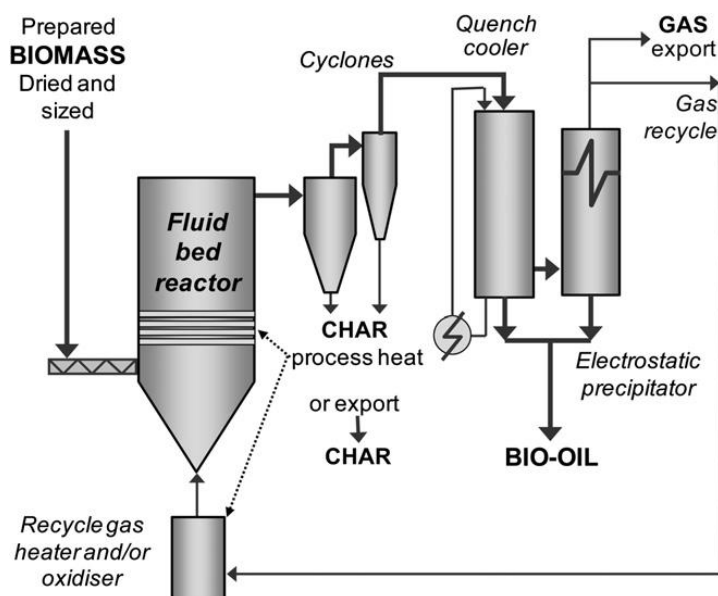


Figure 10. Bubbling fluid bed reactor with electrostatic precipitator.²⁶

Products Obtained From Thermochemical Biomass Routes

Liquefaction products

Liquefaction products in general have lower oxygen content than that from pyrolysis oil. Products obtained from the liquefaction of legume straw, corn stalk, cotton stalk, and wheat straw can be seen in figure 11. Gaseous components ranged from 37.9 to about 52% with carbon dioxide as the dominant component of 81-87%. The majority of the remaining gas product was split between hydrogen and carbon monoxide. Oil yields were relatively low in this study accounting for just 5.2-10.5% of the products. However, the oxygen content of the oil is reduced to a low level of just 5.5-8.6 wt.% from 48.6-52.9 wt.% and a corresponding increase in the HHV from 12-14 to 41-44.4 MJ kg⁻¹.

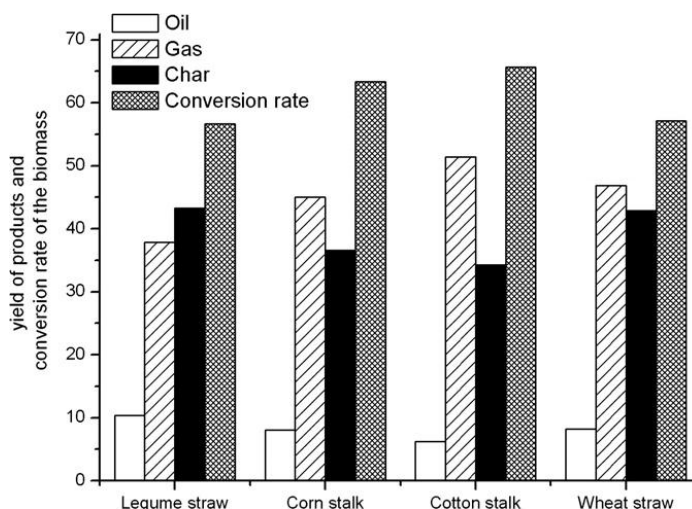


Figure 11. Yield of products during liquefaction of some biomass samples.²⁸

Analysis of the bio-oil was conducted with a GC/MS and grouped into three main components based upon residence time for Benzene derivatives, phenol derivatives, and long chain alkanes. There were hundreds of samples identified with molar concentrations of less than 1-2% such as toluene(1.33%), phenol(1.89%), 3-ethylphenol(2.30%), thymol(3.96%), hexadecane(4.91%) in legume straw. The product compositions varied slightly from one sample to another. It is important to note that the low oxygen content oil is more suitable for direct use or only slight modification as a fuel. Therefore, this review will focus mainly on the pathway for upgrading bio-oil from pyrolysis reactions.²⁸

Pyrolysis products

There can be more than 300 compounds in pyrolysis oil with a high oxygen content of 28-40 wt.% Some of the types of compounds found include carboxylic acids, esters, furans, phenolics, hydroxylaldehydes, and hydroxyketones. The bio-oil is a highly acidic fraction composed of a large amount of water (15-30 wt.%) and highly reactive organic compounds. The low pH of bio-oil causes corrosion problems which need to be considered when constructing pipes and reactors of different metals.²⁷

Innovative work by Ben and Ragauskas shows the percentage of carbon involved in different bonds for the pyrolysis of softwood kraft lignin at various temperatures. It

was shown that aromatic and aliphatic carbon-oxygen bonds were reduced while aliphatic carbon-carbon bonds and aromatic carbon-hydrogen bonds were formed when compared to the original biomass.²⁹

Bio-oil does not mix with any hydrocarbon liquids as it is composed of many oxygen containing groups which cause it to be polar. Alcohols such as methanol and ethanol will dissolve the bio-oil, water will form an emulsion up to about 30% while nonpolar compounds are not miscible. The higher heating value (HHV) of bio-oil as produced is similar to the original biomass at 16-19 MJ kg⁻¹ and still far from that of crude oil (44 MJ kg⁻¹). In order to increase the heating value and decrease the acidity of bio-oil is through removal of water and reduction of oxygen containing groups such as alcohols and methoxyls found in such compounds as guaiacol. But due to the reactive nature of bio-oil, simply evaporating the water through boiling will result in polymerization of the organic species producing a solid residue of around 50 wt.% of the original liquid. Care must therefore be taken in selecting the catalytic routes for upgrading the bio-oil and separating the water fraction. Intermediate steps are used to transform bio-oil into a more stable product which could be introduced into a traditional petroleum refinery where further deoxygenation and separations could take place. The figure below shows a general schematic for the pyrolysis of biomass and upgrading of the bio-oil. The process for upgrading can be as varied as the type of pyrolysis unit used.^{26,27}

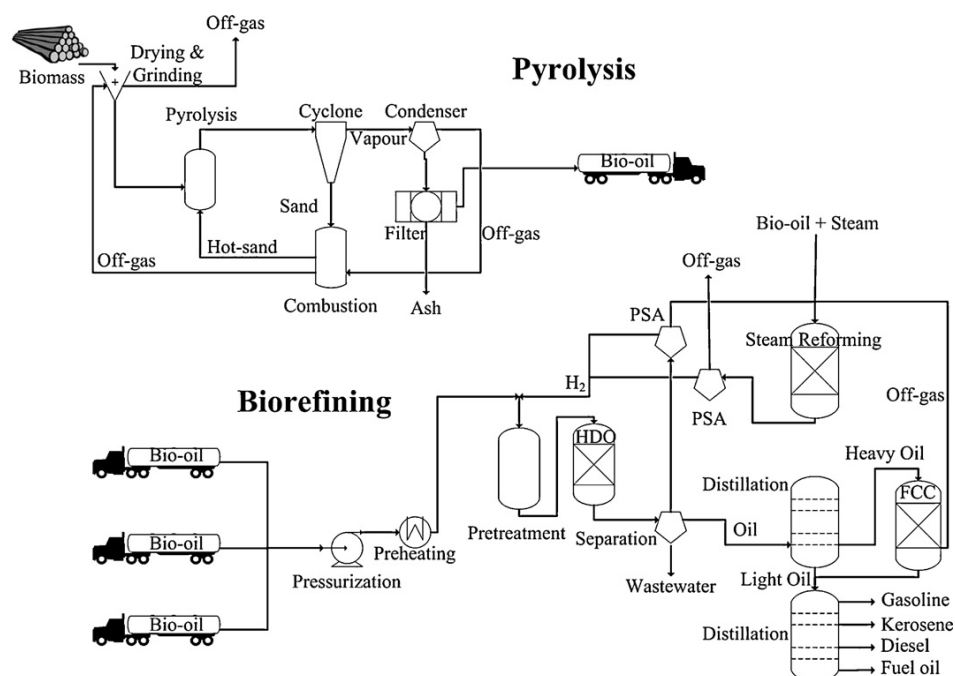


Figure 12. Flow sheet for production of bio-fuels through pyrolysis and catalytic upgrading.²⁷

Types of Upgrading

Physical methods

Reduction of the bio-oil concentration with an alcohol such as methanol will reduce the viscosity while preventing slow secondary reactions from occurring which contribute to an increase in the viscosity over prolonged time. However, these oxygen containing solvents would need to be separated later or upgraded causing greater consumption of hydrogen during hydrodeoxygenation.

Filtration may be used to decrease the amount of ash to less than 0.01 wt.% and alkali content to less than 10 ppm but does not remove any oxygen containing groups which contribute to the acidity of the bio-oil. Removal of the alkali metals such as potassium and sodium will help during catalytic conversion by removing these catalysts which may cause unwanted side reactions.^{26,27}

Hydrodeoxygenation

Also known as hydrotreating, hydrodeoxygenation removes oxygen in the form of water by catalytic reaction with hydrogen in either gaseous form or as a hydrogen donating solvent such as tetralin, sodium formate, or formic acid.¹⁸ Hydrodeoxygenation includes a number of other reactions such as hydrogenation, cracking, and decarboxylation.³⁰ Hydrodeoxygenation can be a very expensive process due to the temperature and pressure requirements to deoxygenate of 300-400°C with hydrogen pressure up to 200 bar. However, aromatic structures such as benzene, toluene, and xylene can be preserved which yields a high octane fuel.³¹ Due to the reactive nature of bio-oil at temperatures above 373 K, two-step hydrotreating processes for upgrading pyrolysis oil to transportation fuel has been suggested to reduce the reactivity at less than 573 K in the first stage by reduction of the most reactive species like ethers, methoxyphenols, aldehydes, and ketones. The second stage of hydrotreating would be at a higher temperature to remove most of the remaining oxygen species. Elliott and Baker performed this two stage reaction at 573 K and 626 K on bio oil to decrease the oxygen content from 52.6 wt.% to 32.7 and 2.3 wt.% over a CoMo/Al₂O₃ catalyst.³² For detailed reaction kinetics, model compounds have been used to elucidate the mechanism of oxygen removal in various systems. Most model compound studies of hydrodeoxygenation involve a nonpolar organic solvent with low concentrations of bio-oil model compounds such as furan, benzofuran, bibenzofuran, phenol, guaiacol, or acetic acid.^{26,27,33,34} These types of reactions will be reviewed later.

Zeolite Cracking

Zeolite cracking is the use of high temperatures without hydrogen in the removal of oxygen as water or carbon dioxide. Despite the advantages of not using hydrogen, the acid sites of the catalyst are easily coked thus preventing prolonged catalytic reactivity.

Typical reaction temperatures range from 300 to 600°C using a number of different zeolites as shown below in table 1. In general, higher temperatures result in greater deoxygenation with increased gas yields and reduced oil yields by balance.^{26,27}

Table 1. Zeolites used for catalytic cracking of pyrolysis oil or model compounds and reaction temperature.

Williams & Horn ³⁵	HZSM-5	Bio-oil	400-550°C	1994
Adjaya & Bakhshi ³⁶	HZSM-5	Bio-oil	330-410°C	1994
	Silicate			
	H-mordenite			
	HY			
	SiO ₂ -Al ₂ O ₃			
Samolada, et al. ³⁷	ReUSY ₁	Bio-oil	500-550°C	1998
	ReUSY ₂			
Huang et al. ³⁸	HY ₁	Model comp.	rt-500°C	2009
	HY ₂			

Hydrodeoxygenation Catalyst Review

Initial work performed on the hydrodeoxygenation of pyrolysis oil involved borrowing of the sulfided CoMo or NiMo on alumina catalysts from the oil industry where they are used for hydrodesulfurization (HDS) and hydrodenitrogenation (HDN) reactions. However, due to the limited amount of sulfur in bio-oil, gaseous sulfur had to be added or else the catalyst would lose activity. These catalysts work well and are capable of deoxygenating compounds without hydrogenation of aromatic rings, but the need for sulfur added to the costs as well as introduced more of the element into the fuel. A brief summary of some catalysts studied for hydrodeoxygenation reactions are shown in table 2. It was later realized that the instability of alumina supports in the presence of hot water would need to be addressed.³⁹ While researchers have noted the problems with γ -Al₂O₃ supports, there are still studies being performed today.

Batch studies performed by Gevert & Otterstedt⁴⁰ in the late 1980's performed hydrodeoxygenation of a bio-oil in solution with decalin. It was shown that temperature had the largest effect on converting the highest boiling point reactants into naptha and gas

oil products with a CoMo catalyst. Yields increased linearly from 52 to 65 wt.% with increases in temperature from 325 to 390°C with little variation due to hydrogen pressure. Gas yields increased with temperature but were less than 2 wt.% at 390°C and 150 bar of hydrogen. Later work by Baldauf et al.⁴¹ investigated the effects of temperature, space velocity, reactor flow (up or down), and two sulfided catalysts on the conversion of bio-oil. It was found that harsh conditions resulted in near complete removal of oxygen containing species while increases in water yield from 21-25.5 wt.% were observed. The hydrodeoxygenated oil fraction decreased from 36.3 to 32.2 wt.% as the degree of oxygen removal increased from 88.3 to 99.9%. This corresponded to variations in the HHV of the oil fraction between 41.2 and 45.96 MJ kg⁻¹, signifying a large increase in the typical heating value of 16-19 MJ kg⁻¹ of bio-oil. Extended reactions were performed in the downflow configuration which had to be terminated due to plugging caused by decreased catalytic activity which allowed the formation of polymerized species.^{40,41}

Table 2. Hydrodeoxygenation (HDO) catalysts, supports, and years of publication.

Gevert et al. ⁴⁰	CoMo	γ -Al ₂ O ₃	1987
Baldauf et al. ⁴¹	CoMo, NiMo		1994
Elliott ³⁹	Pd, Ru	Carbon	2009
Elliott & Hart ⁴²	Pd/C	Carbon	2009
Hong et al. ⁴³	Pt	HY, H β , HZSM-5, Al ₂ O ₃ , SiO ₂	2010
Nimmanwudipong ⁴⁴	Pt	γ -Al ₂ O ₃ & HY Zeolite	2011
Bui et al. ⁴⁵	MoS ₂ , CoMoS	γ -Al ₂ O ₃ & unsupported	2011
Wang et al. ³³	Pt	Al ₂ O ₃ , ZSM-5, mesopore ZSM-5	2011
Joshi & Lawal ³¹	NiMo	Al ₂ O ₃	2012

More recent work involves the use of noble metal catalysts for the hydrodeoxygenation of bio-oil as seen in the table above. Elliott and Hart treated model compounds of bio-oil in water with palladium or ruthenium on carbon in a high hydrogen pressure reactor at 150, 200, 250, and 300°C. At 200°C over ruthenium catalyst, guaiacol is hydrogenated to 2-methoxycyclohexanol and to a lesser degree, cyclohexanol with

several other minor components. At 250^oC, cyclohexanol is a major product after 1 hour at temperature before later being converted to cyclohexane. Acetic acid showed little inclination to react until 250^oC when ethanol was found at similar concentrations to that of the acid and nearly none remained after 4 hours of reaction. 96% of the acid was converted and just 4% of the ethanol remained showing that further reaction to methane and water occurred. Palladium did not have the same results as ruthenium and showed a large amount of gas products after reaction of guaiacol. After 4 h at 300^oC, 20% ethanol was formed from the acetic acid with little gasification. Therefore, ruthenium hydrodeoxygenated guaiacol faster and produced gases upon reaction of acetic acid at 250^oC while palladium gasified guaiacol products and converted acetic acid to ethanol with a few percent ethyl acetate.³⁹

Work by Do-Young Hong et al.⁴³ explored the use of Pt supported on HY zeolite for the conversion of a bio-oil model compound phenol at varying temperature and space velocity. At 473 K and after 2 h on-stream with varying space velocities, it was shown that at complete conversion of phenol, cyclohexane was the largest product at over 95%. The selectivity of cyclohexane was still greater than 60% even at low conversion of phenol. Cyclohexanol peaked at the lowest conversion of phenol and rapidly degraded while cyclohexanone subsequently increased and later decreased with further severity. Cyclohexenol was observed at very low conversions alluding to the intermediate product between cyclohexanol and cyclohexanone. A conversion plot and the proposed reaction pathway for this reaction are given below. The authors also observed formation of several different bicyclic compounds exhibiting selectivities of less than 5%. While these are not major products in this work, polymerization of actual bio-oil products could be a major concern with increased loading.⁴³

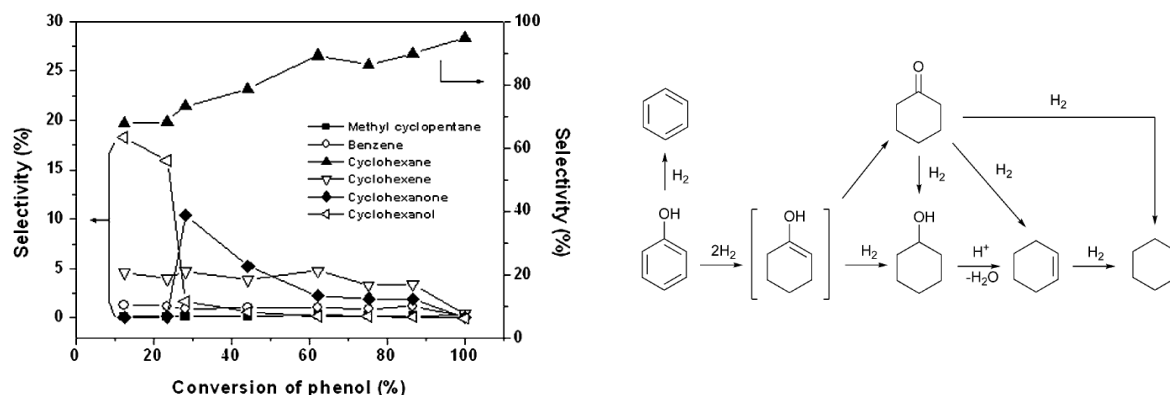
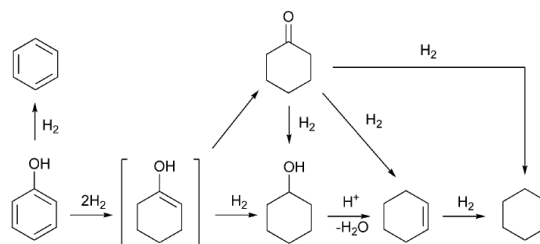


Figure 13. Selectivity vs. phenol conversion for Pt/HY zeolite at 473 K; H_2 pressure, 4 MPa; WHSV, $5\text{--}20\text{ h}^{-1}$; 2 h reaction time.⁴³

Scheme 1. Reaction pathway of phenol with Pt/HY zeolite catalyst.⁴³



Hydrodeoxygenation Support Review

Further work by Hong et al. investigated the role of supports used in the conversion of aqueous phenol over Pt catalysts. The limited data shows at 523 K, weighted hourly space velocity (WHSV) of 20 h^{-1} , 4 MPa H_2 , Pt on HY, H β , and HZSM-5 zeolites are converted to cyclohexane with 93.7, 94.7, and 89.7% selectivity while Pt on Al_2O_3 and SiO_2 are 93.38 and 94.62% selective to cyclohexanol at 473 K. The authors conclude that acidic protons are required for the dehydration of phenol coupled with a metallic function to hydrogenate the aromatic ring.⁴³ While tests were not conducted for long periods of time, it is believed that activity would decrease with time due to the high temperature water forming hydroxyl units on the support surface as noted in other works.²⁷

Mesoporous ZSM-5, HZSM-5, and alumina were investigated with 0.5 wt.% Pt loading for the conversion of a large model compound dibenzofuran (DBF) in n-tridecane in a continuous flow, fixed bed reactor. Both zeolites showed greater acidic strength than alumina based upon NH_3 -TPD, bulky amine chemisorptions and model catalytic reaction. At a liquid hourly space velocity (LHSV) of 2 h^{-1} , all catalysts performed well at deoxygenating DBF, but quickly lose this ability at higher liquid space velocities as seen in figure 14. The proposed reaction pathway of dibenzofuran is shown in scheme 2. At a

LHSV of 6 h^{-1} , the mesoporous Pt catalyst is nearly fully converted to BCH and CPM-CH, 83.4 and 14.9% selective. The alumina support provides sufficient hydrogenating ability but lacks the acidity to dehydrate BCH-3-en-2-ol, whereas the ZSM-5 support possesses higher acidity to remove oxygen containing groups but suffers hydrogenation capacity due to diffusion limitations of DBF in the microporous structure. The hydrogenation of the mesoporous zeolite is achieved faster and the acidic protons rapidly dehydrate the DBF products.³³

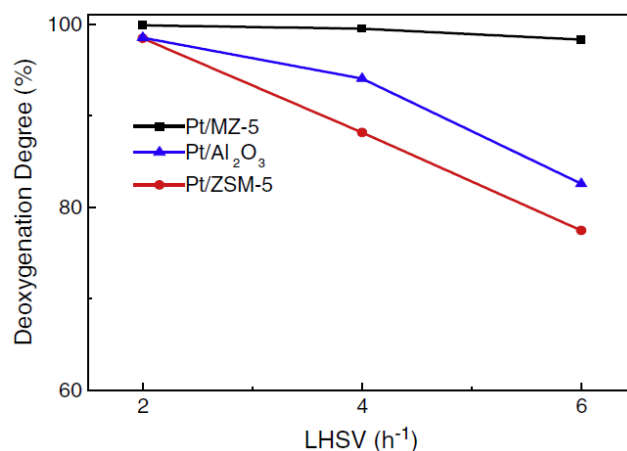
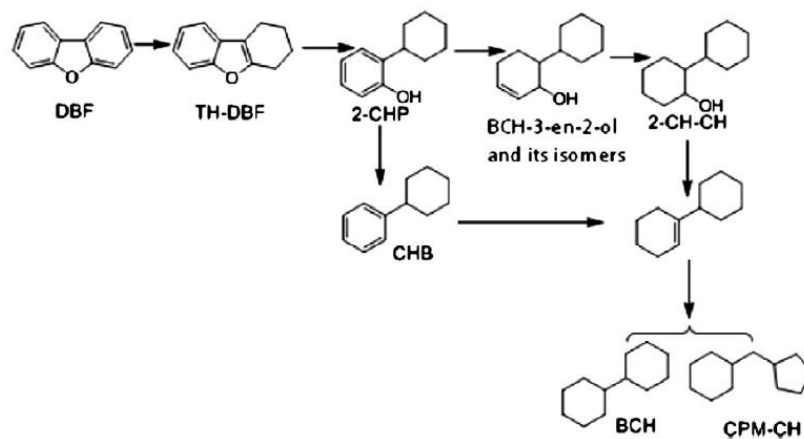


Figure 14. Dibenzofuran (DBF) deoxygenation degree at varying LHSV.³³



Scheme 2. Schematic expression of the DBF reaction pathway.³³

The above reaction scheme seems plausible considering the high bond dissociation energies of aromatic C-O bonds compared to aliphatic C-O bonds. Table 3 shows the bond dissociation energies for oxygen containing groups.³² From the table, the

bond strength of the O attached to the aromatic carbon is about 83 kJ/mol greater than the aliphatic carbon-oxygen bond. The aliphatic bond would then be simpler to break than the aromatic thus justifying part of the reaction pathway proposed.

Table 3.³² Bond dissociation energies (kJ/mol).

RO-R	339
RO-Ar	422
R-OH	385
Ar-OH	468

Hydrodeoxygenation Solvents Review

Solvents are often used in conjunction with model compound studies to isolate a particular element of the bio-oil and elucidate detailed reaction kinetics which may be used to better explain the reaction mechanisms of the bio-oil. Many of the experiments are run in batch liquid phase using polar organic, non-polar organic, or aqueous solvents. In one interesting work by Fisk et al. model compounds were used together in forming a synthetic bio-oil complete with 20 wt.% water and a pH of 2.3. Platinum was selected as the catalyst due to its high activity in cleaving of C-C bonds as well as C-H and/or O-H bonds for the production of H₂ by aqueous-phase reforming (APR).⁴⁶ Many solvents were investigated as seen from table 4 below.

Table 4. Catalysts, supports, model compounds, and solvents used in some hydrodeoxygenation reactions.

Lee et al. ⁴⁷	CoMo	γ -Al ₂ O ₃	Benzofuran	hexadecane
Senol et al. ⁴⁸	CoMo, NiMo	γ -Al ₂ O ₃	Phenol	<i>m</i> -xylene
			Cyclohexanol	
			Benzene	
Echeandia et al. ⁴⁹	Ni-W, Ni, W	Carbon	Phenol	<i>n</i> -octane
Gutierrez et al. ⁵⁰	Rh, Pd, Pt, & more	ZrO ₂	Guaiacol	<i>n</i> -hexadecane
Fisk et al. ⁴⁶	Pt	γ -Al ₂ O ₃ ,	Methanol	(synth. bio-oil)
		TiO ₂	Acetaldehyde	
		ZrO ₂	Acetic acid	
		SiO ₂ -Al ₂ O ₃	Glyoxal	
		CeO ₂	Acetol	
		Ce _{0.7} Zr _{0.3} O ₂	Glucose	
			Guaiacol	
			Furfural	
			Vanillin	
			Deionized water	

The synthetic bio-oil contained 5 wt.% methanol, 12 wt.% acetaldehyde, 14 wt.% acetic acid, 4 wt.% glyoxal, 8 wt.% acetol, 8 wt.% glucose, 17 wt.% guaiacol, 4 wt.% furfural, 8 wt.% vanillin, and 20 wt.% deionized water. The selected model compounds and their proportions reflect the main compound types of typical pyrolysis oils. Catalytic reactions were performed under inert atmosphere at 350°C in a mechanically stirred batch autoclave. In the absence of hydrogen, it would be very likely to see large amount of solid, carbon-rich residues after reaction. From figure 15, we can see a larger yield of solids than oil for many of the catalysts studied. The alumina support had the greatest deoxygenating ability while preserving carbon of the catalysts studied and was investigated further.⁴⁶

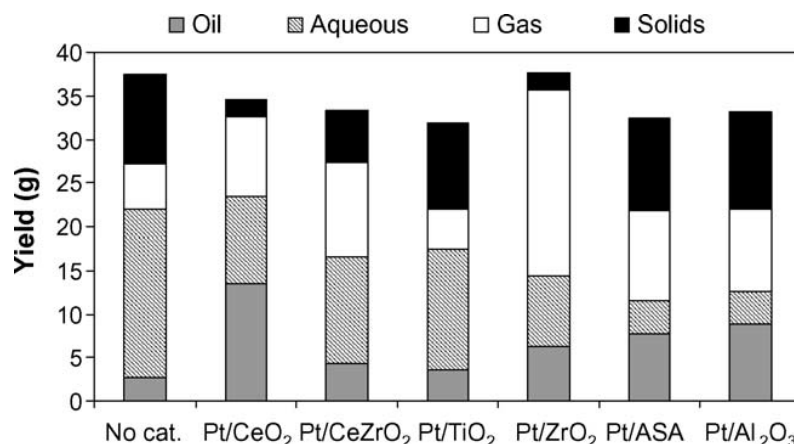


Figure 15. Gas, Liquid, and solid yields from treatment of model bio-oil with Pt catalysts. (Reaction time of 2 h with initial mass of synthetic bio-oil = 40 g)⁴⁶

A second synthetic bio-oil solution was also made which contained no water for tests with Pt/Al₂O₃ at 4 h of reaction instead of the 2 h used with the other catalysts. For the bio-oil containing water, one would expect that the oxygen content would decrease with time for experiments done on a short time scale as the ones shown here. However, when using the bio-oil without water, the oxygen content of the oil produced actually increases as seen in figure 16. The author attempts no discussion as to why this occurred, solely stating that water was “advantageous for deoxygenation”. This result seems to defy convention and may need further investigation.⁴⁶

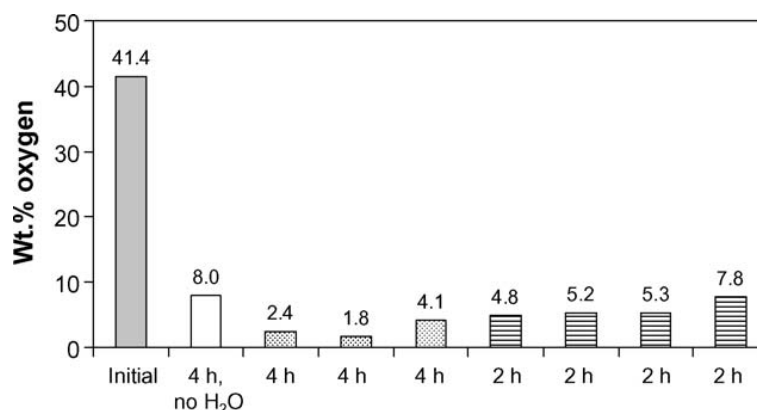


Figure 16. Oxygen content of oil product obtained from treatment of synthetic bio-oil with Pt/Al₂O₃.⁴⁶

Literature Review Summary

Lignin is an undervalued resource in the production of renewable fuels and pyrolysis shows to be an effective method in destroying bonds, one of the keys to transforming lignin into a fuel. The upgrading of bio-oil has required considerable effort from catalysis to transform difficult to break carbon-oxygen bonds and remove the acidic nature of bio-oil while minimizing polymerization reactions. Hydrogen has been identified to reduce the amount of solids formed and hydrodeoxygenation has grown in effectiveness as catalysts, supports, and model compounds have been studied over the years. One area that should be studied is the solubility of hydrogen and the role the solvent plays interacting with catalyst, support, and products from pyrolysis. Little attention has been paid to the solvents role in hydrodeoxygenation reactions.

Hydrogen solubility

Gas solubility data in various solvents is sparse at best. The most common solvent in the literature is water at temperatures not far removed from 298 K. Determination of the solubility in other solvents necessitates the use of equations of state, fugacities, or other related thermodynamic calculations of which data may not exist at the temperature and pressure desired. Thus, we compared the hydrogen solubility at 25⁰C for both of our solvents and were fortunate enough to find data for both. According to Perry's Handbook, the molar ratio for hydrogen in water at 298 K and 1 atm is 1.413E-05 yielding a concentration of 1.565 g H₂ m⁻³.⁵¹ The molar ratio for hydrogen in heptane at similar conditions is between 3.98E-04 and 6.88E-04, resulting in a concentration of hydrogen of 5.44 - 9.404 g H₂ m⁻³.⁵² Therefore, at the starting temperature, heptane may allow 3.5 – 6 times the concentration of hydrogen than water. Indeed, these estimations agree well with another work comparing hydrogen solubility in aqueous and different organic solvents.⁵³

CHAPTER 2

HYPOTHESIS & OBJECTIVES

Hypothesis for Catalytic Hydrodeoxygenation (HDO) Reaction

It is well known that an increased hydrogen concentration in solution will increase the reaction rate. Because hydrogen solubility in non-polar solvents is much higher than in water and alcohols at normal conditions, it is our belief that hydrodeoxygenation of bio-oil can be significantly improved by using non-polar organic solvent as the reaction medium. We also believe that Henry's law should prevail and that by increasing the hydrogen partial pressure, there will be a corresponding increase in the concentration of dissolved hydrogen at similar reaction temperatures.

Objectives

- Compare the hydrodeoxygenation ability of a bio-oil model compound in aqueous and organic solvents with Pt/C catalyst at constant volume concentration and same reaction conditions (temperature and hydrogen pressure).
- Study the hydrodeoxygenation of model compound with different pressures and temperatures with Pt/C catalyst
- Determine the reaction scheme by quantitatively analyzing the experimental results.
- Determine whether hydrogen solubility or solvent-catalyst interactions may be limiting reaction.

CHAPTER 3

EXPERIMENTAL

Analysis Methods

UV-Vis

Ultraviolet-visible spectroscopy was used to quantitatively determine the changes in pi bond concentrations from the original model compound. By using the Beer-Lambert law, which states that absorbance is directly proportional to the concentration of probed species, we can create a known concentration curve to compare samples against in order to determine their concentration based on the measured absorbance. Figure 17 shows three known concentrations plotted against absorbance. The curves appear identical before and after reaction in this region. Pi electrons are able to absorb ultraviolet or visible light by transferring this energy to an excited state. The wavelength of light absorbed depends upon the adjacent groups and other double bonds in conjugation as well as the solvent used. Guaiacol shows a clear maximum wavelength at 274 nm or 275-276 nm for water and heptane solvents, respectively. From the standards, a linear equation could be fitted based on concentration versus absorbance at a similar wavelength. The samples could then be run and based on their dilution and absorbance, their concentration could be determined.

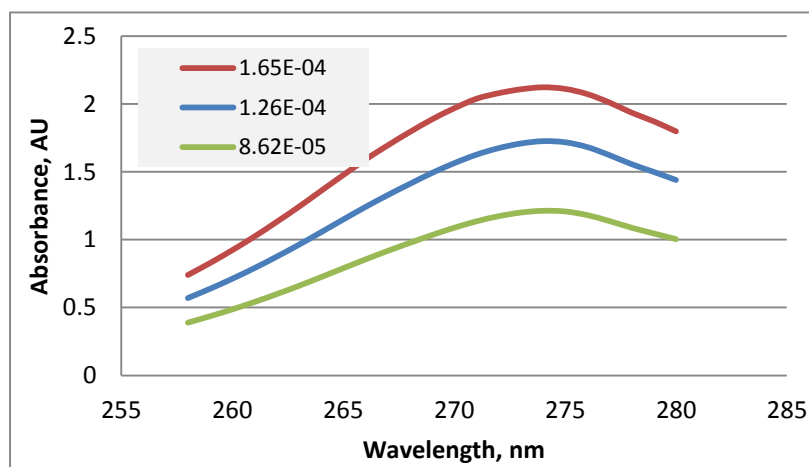


Figure 17. UV-Vis of three standard guaiacol solutions in water. Peak absorbance at 274nm. Weighted concentrations shown in table.

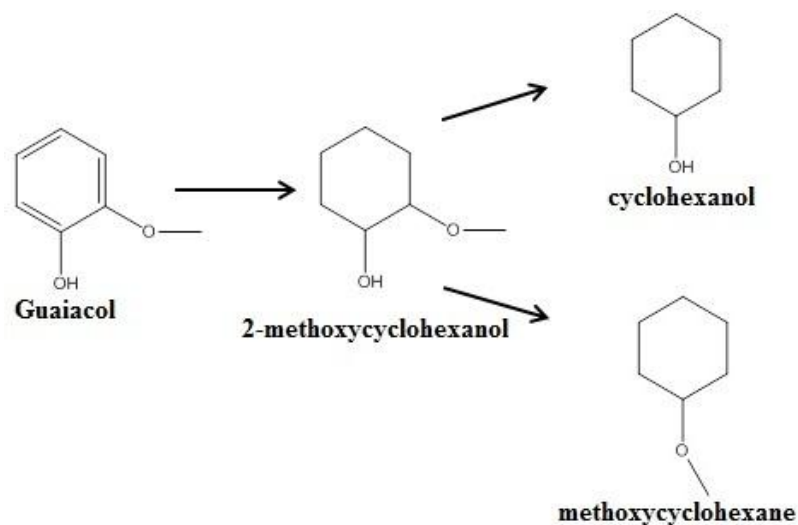
GC-MS

Gas chromatography-mass spectrometry combines the separating ability of the gas chromatograph with the mass spectrometer to identify individual compounds based on their molar mass and fragmentation pattern. Different molecules from a sample will take different amounts of time to travel through the column depending upon the size and interaction of the molecules with the properties of the column. Once out of the column, the mass spectrometer bombards the molecules with electrons which can cause loss of an electron and break apart the sample in a predictable fashion. The charged particles are then accelerated out of the ionizing area by electromagnets and sent around a curved trajectory hitting a detector which counts the number of collisions while measuring the magnetic strength in order to determine the size of the ions. Larger ions will take a longer arc than smaller ones with a given electromagnetic strength applied to influence their velocity. Based on the fragmentation pattern, the computers database compares the sample with a set of standards to determine the structure of the unknown. GC-MS is usually not considered a quantitative analytical tool, but with comparison to the UV-Vis it tends to agree well with the heptane solvent reactions.

Materials and Reaction Conditions

A Parr model 4593 reactor was used for all experiments with a glass sleeve manufactured at the Georgia Tech Glass Workshop. The total internal volume of the reactor is calculated to be ~80 cubic centimeters. 5% Platinum on carbon from Aldrich, 99+% heptane from Sigma-Aldrich, Nanopure deionized water, 98+% 2-Methoxyphenol (Guaiacol) from Alfa Aesar, Ultra-High purity Hydrogen from Airgas, and Aluminum Chloride Hexahydrate from J. T. Baker were used as received without further purification. Heptane was used during experiments for its similarity to gasoline type fuels. Chemicals were measured into the glass sleeve such that the guaiacol volume concentration was 0.625% and the mass concentration of catalyst to modeling compound was 10%. The reactor was then purged with hydrogen for 2 minutes while mixing to remove oxygen and nitrogen. Hydrogen gas was then filled to the desired starting pressure of 17.2 or 34.5 barg (250 or 500 psig) and the reactor sealed. The standard Parr impeller was used for all tests at 250 rpm. The heater was then turned on which had a heating rate of about 18 K min^{-1} with a 2 or 3 minute delay response for heptane or water, respectively. Reaction time began once the reactor reached the setpoint temperature of 393, 443, 493, or 523 K. The normal reaction time was three hours, but tests were done varying time at 250 psig and 250°C for 1, 3, and 10 hours. The reactor was quenched in water at the end of the reaction to quickly stop it and bring the temperature below 373 K in less than 5 minutes. The reactor was equilibrated until the temperature maintained at less than 305 K and gases were vented without capture. Typically, more than 90% by mass was recovered and stored in a sealed glass sample bottle with aluminum foil cover in a fridge at 5°C until analysis could be performed.

The possible hydrodeoxygenation reactions of guaiacol and hydrogen at the above conditions are shown below in scheme 3.



Scheme 3. Proposed reaction pathway for the hydrodeoxygenation of guaiacol with Pt/C catalyst.

Results

It can be shown that the solvent has a marked impact on the conversion of lignin model compound guaiacol. Conversion is calculated according to equation 1. It may be converted to one of several products shown above. The heptane solvent clearly allows greater conversion to products with the aid of platinum on carbon catalyst as seen in figures 18 and 19.

Equation 1

$$\text{Conversion} = \left(\frac{C_i - C_f}{C_i} \right)$$

Where C_i is the initial concentration of guaiacol and C_f is the final concentration of guaiacol as measured by UV-Vis comparing to a calibration standard set.

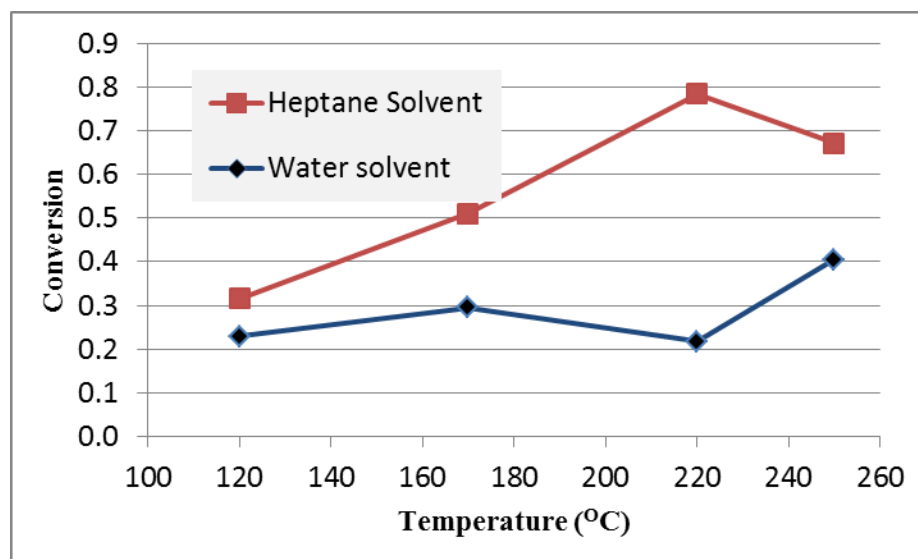


Figure 18. Comparison of guaiacol conversion at 250 psig, 3 hr reaction time at varying temperature for heptane and water solvents.

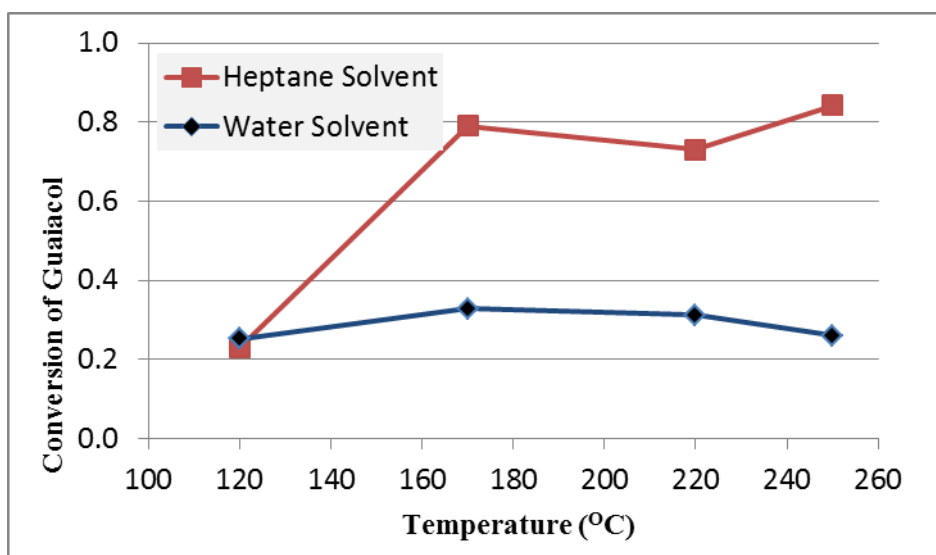


Figure 19. Comparison of guaiacol conversion by UV-Vis at 500 psig, 3 hr reaction time at varying temperature for heptane and water solvents.

A difference in doubling the pressure was less dramatic than differences in temperature and between the solvents used. The maximum conversion at 250 psig and 3 hours was 78.4 and 40.5% for heptane at 493 K and water at 523 K, respectively. The conversion decreased in the water solvent at elevated pressure to just 32.9% at 443 K while increasing to 84.2% at 523 K for heptane solvent. Comparison of the pressures for

each solvent can be seen in figures 20 and 21. Assuming that the concentration of hydrogen in the solvent should be proportional to the partial pressure, we would expect to see an increase in the conversion to products if the concentration of hydrogen is rate limiting. However, from the data we can see no significant differences by doubling the pressure. Therefore, other factors must contribute to the hydrogenation and deoxygenation of guaiacol in solvent.

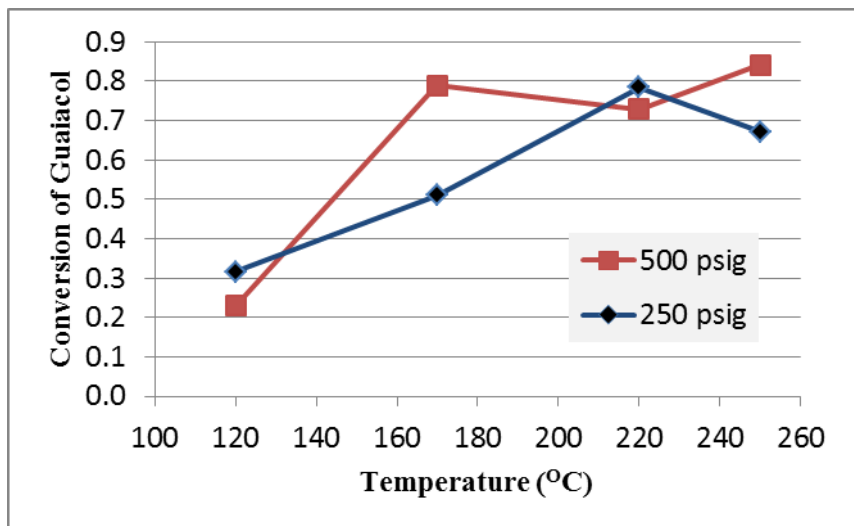


Figure 20. Guaiacol conversion at varying temperature and pressure in heptane solvent at 3 h by UV-Vis.

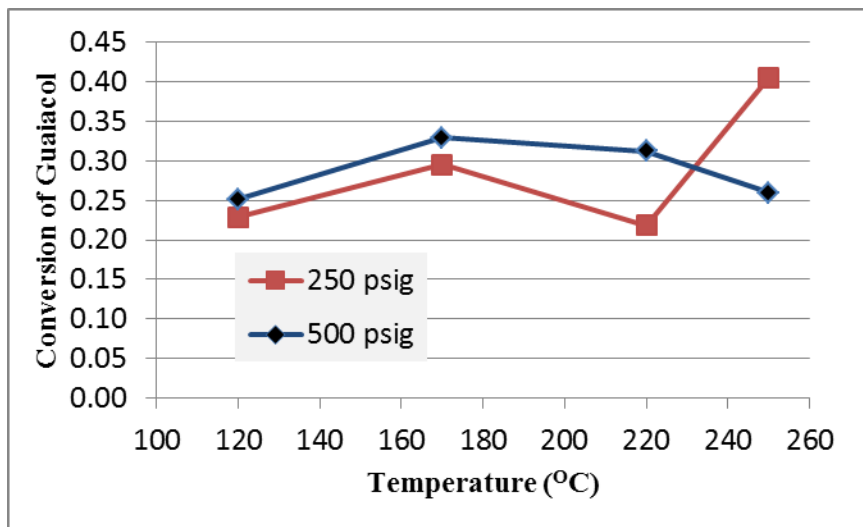


Figure 21. Guaiacol conversion at varying temperature and pressure in aqueous solvent at 3 h by UV-Vis.

It is theorized that differences in hydrogen solubility and the catalyst surface – solvent interactions are resulting in the differences in conversion observed. Figure 22 shows the conversion in both solvents with time at temperature of 523 K and 250 psig. It is observed that both solvents show near complete conversion at the longest time of 10 h. The data appeared contaminated at 1 h and is not shown.

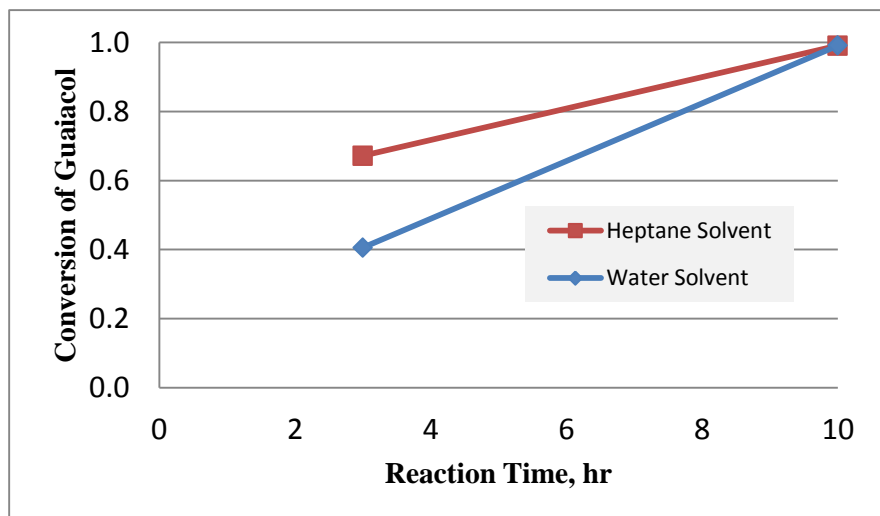


Figure 22. Comparison of solvents with time at 250 psig and 250°C by UV-Vis.

GC-MS was later used to determine the agreement with UV-Vis data and establish products of the reaction. Heptane solvent reactions were merely filtered before sampling at the GC-MS and show very good agreement with overall conversion as seen in figures 23 and 24. Agreement between techniques was not observed after extraction of organic constituents from aqueous solvent with chloroform as seen in figure 25. A similar outcome was seen for the lower pressure water solvent. The extraction was deemed necessary for the aqueous reactions to ensure complete volatilization inside the GC-MS. Water is not as effective as chloroform in the GC-MS so ca. 2 mL of chloroform was added to ca. 5 mL of water products and mixed well. The chloroform was drawn into a syringe and forced through a 40 micron filter. Differences in the solubility of the products between the chloroform and water caused the conversion to be skewed when comparing

the GC-MS data to the UV-Vis. Because the UV data was not altered to sample, it should be considered the more accurate of the two tests for the water reactions. The long duration water GC-MS sample might be fair to use to get a general idea of the products obtained from the complete conversion of guaiacol due to fewer compounds extracting into the chloroform.

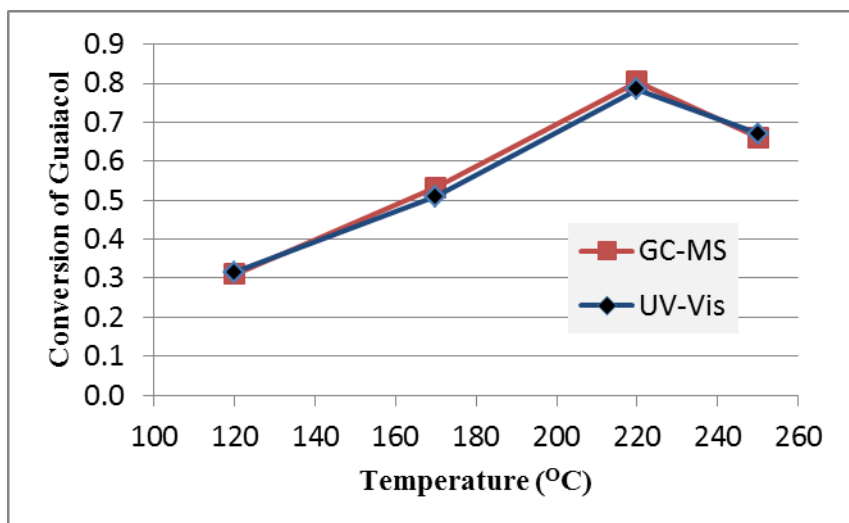


Figure 23. Analytical measurement comparison for heptane solvent at 250 psig and 3 h.

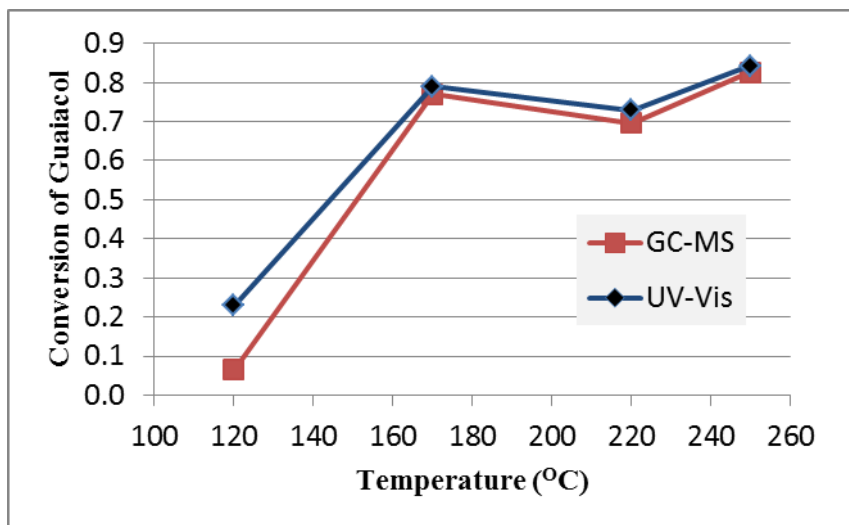


Figure 24. Analytical measurement comparison for heptane solvent at 500 psig and 3 h.

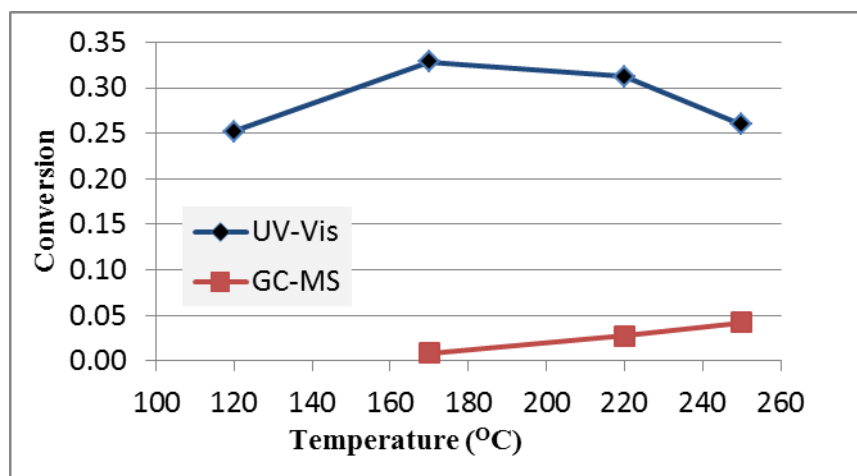


Figure 25. Conversion comparison of analytical measurements for water solvent at 500 psig and 3 h.

By showing good agreement between the two analytical techniques for the concentration of guaiacol in heptane solvent, the products concentration could then be used with reasonable clarity. However, we cannot utilize GC-MS results for nearly all of the reactions which occurred in water solvent due to vast differences observed in conversion. Differences in solubility of the compounds formed should contribute to differences between the two tests for the aqueous reactions.

Four primary compounds were detected by the mass spectrometer database as guaiacol, 2-methoxycyclohexanol, methoxycyclohexane, and cyclohexanol as seen below.

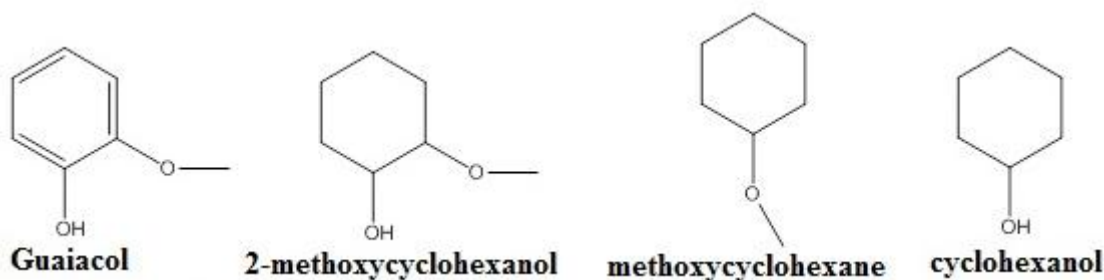


Figure 26. Hydrodeoxygenation products observed from the GC-MS.

The single largest product is simply the hydrogenation of the aromatic ring as evident in figures 27 and 28. No aromatic ring with one or both oxygen containing groups

removed was observed, alluding to the mechanism that removal of oxygen containing groups occurs after hydrogenation of the pi bonds.

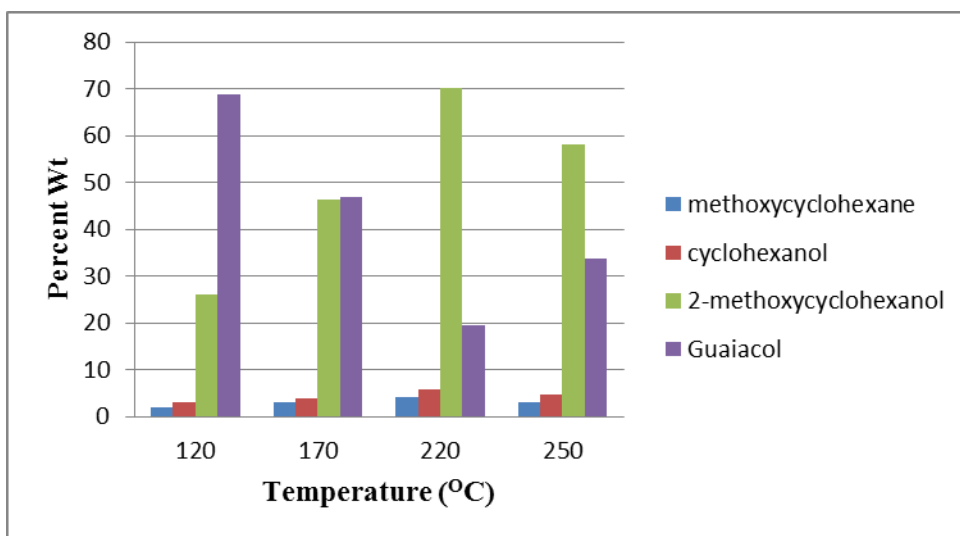


Figure 27. Products from guaiacol, identified by GC-MS, in heptane at 250 psig for 3 hours.

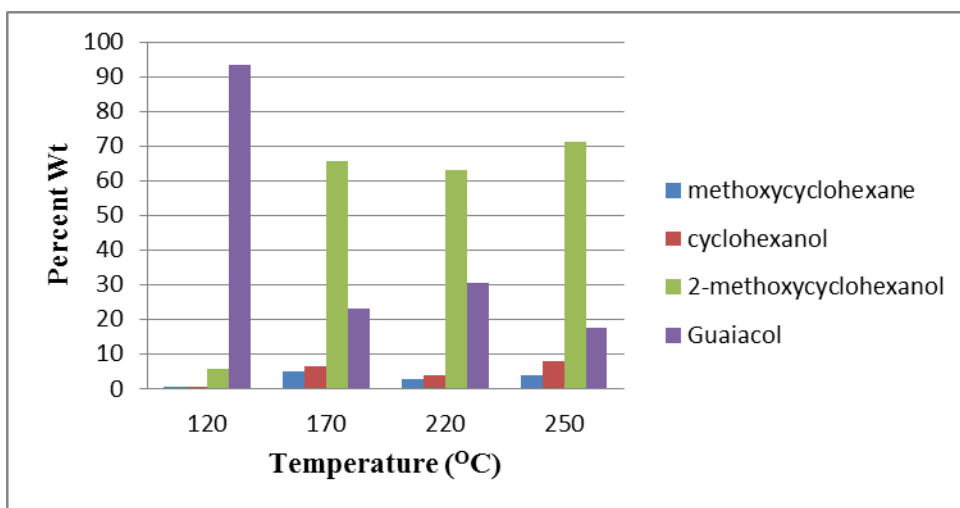


Figure 28. Products from guaiacol, identified by GC-MS, in heptane at 500 psig for 3 hours.

There is consistently a higher concentration of cyclohexanol over methoxycyclohexane. Thus, it can also be concluded that the bond strength between the methoxy group and ring is weaker than between the alcohol group and ring.

From figure 29, we can see that the reaction proceeds quite rapidly at first and slows considerably. The conversion is nearly identical between 1 and 3 hours of reaction time at ~65%. This could be caused by a low concentration of model compound showing difficulty in adsorbing onto the catalyst surface due to a number of reasons.

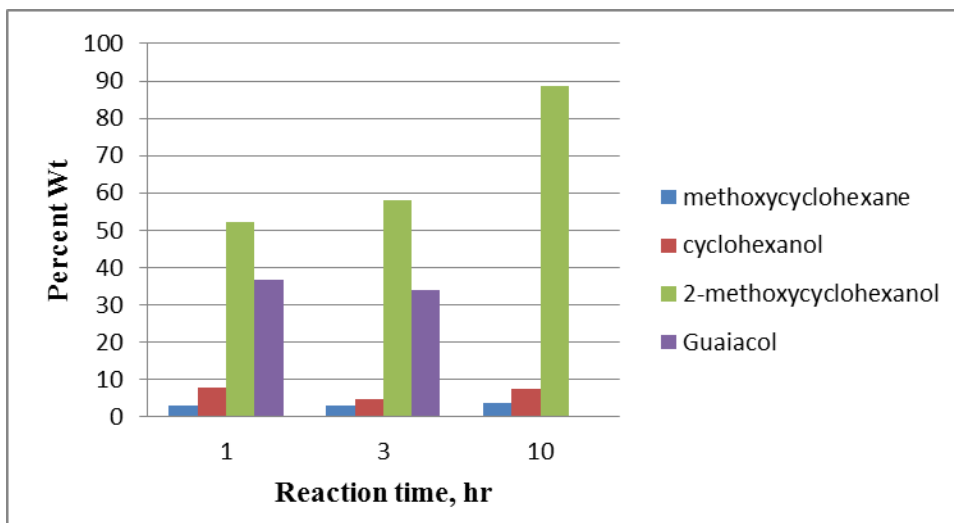


Figure 29. Reaction products via GC-MS at 250 psig H₂ and 250°C in heptane for various times.

Previous work on the hydrodeoxygenation of phenol in water solvent with palladium on carbon catalyst showed a reaction pathway first hydrogenating the aromatic ring followed by an acid catalyzed two step removal of the alcohol group to form cyclohexane.⁵⁴ They could show no evidence of direct hydrogenolysis in removing the oxygen containing group with their catalyst and could extend this work for other catalysts like platinum, ruthenium, and rhodium. Similarly, we have no evidence of direct removal of oxygen containing groups or formation of carbonyl groups prior to hydrogenation of the aromatic ring. Our reactions pathway follows a similar route.

CHAPTER 4

SUMMARY

Conclusion

Heptane is shown to be an effective solvent for the hydrogenation of a lignin model compound when compared to aqueous solvent. The maximum conversion was 40.5% in water at 250⁰C for 3 hours while the same conversion can be achieved in heptane between 120 and 170⁰C at the same amount of time and hydrogen pressure. It is believed that an increased hydrogen solubility of heptane with respect to water is helping attribute to the conversion of guaiacol to 2-methoxycyclohexanol. Direct deoxygenation of either oxygen containing groups is also not observed with the catalyst chosen. It is also shown that further conversion to cyclohexanol or methoxycyclohexane is not catalyzed by the reaction system we have used. Other work⁵⁴ has suggested this further conversion is based upon an acid catalyzed intermediate step. Degraded lignin fragments could be used during the conversion of gasoline, diesel and other fuels to supplement fossil fuels with renewable lignin.

It is also shown that increased hydrogen pressure does not increase conversion in the anticipated manner, suggesting other aspects are playing a role in the reaction. This may be due to concentration gradients between solution and that adsorbed onto the catalyst surface.

Recommendations for Future Work

We have seen that increasing the hydrogen pressure does not lead to significant enhancements in the conversion of guaiacol. This could be due to the solubility of hydrogen not relating to adsorption onto the catalyst surface in an obvious way. It would

be very insightful to learn the actual concentration of hydrogen in solution and on the catalyst surface at reaction conditions.

The use of hydrogen donating solvents such as tetralin, formic acid, or sodium formate are interesting avenues to look at. Care must be observed though as generation of hydrogen and other gases might cause the reactor to go beyond its allowable operating pressure. One challenge of hydrogen donating solvents is the need to constantly purchase these solvents. Therefore, generation of hydrogen from the bio-oil itself could prove to be a unique opportunity with the correct catalyst, support, and perhaps solvent system.

REFERENCES

- [1] U.S. Energy Information Administration DOE/EIA-0035(2012/05) Monthly Energy Review - May 2012
- [2] U.S. Energy Information Administration DOE/EIA-0384(2010) Annual Energy Review 2010 – October 2011
- [3] J. R. Franks, B. Hadingham, *Land Use Policy* **29** (2012) 727-736
- [4] D. Iribarren, J. F. Peters, J. Dufour, *Fuel* **97** (2012) 812-821
- [5] P.A.J. van Oort, B.G.H. Timmermans, A.C.P.M. van Swaaij, *Eur. J. Agron.* **40** (2012) 102-111
- [6] M. Lenzen, R. Schaeffer, *Climatic Change* **112** (2012) 601-632
- [7] M. Biasutti, A.H. Sobel, A.J. Camargo, T.T. Creyts, *Climatic Change* **112** (2012) 819-845
- [8] IPCC, 2007: *Climate Change 2007: Synthesis Report. Contribution of Working Groups I, II and III to the Fourth Assessment Report of the Intergovernmental Panel on Climate Change* [Core Writing Team, Pachauri, R.K. and Resisinger, A. (eds.)]. IPCC, Geneva, Switzerland, 104 pp.
- [9] J. Zakzeski, P.C.A. Bruijninx, A.L. Jongerius, B.M. Weckhuysen, *Chem. Rev.* **110** (2010) 3552-3599
- [10] M. Parikka, *Biomass Bioenerg.* **27**, 613 (2004)
- [11] A.J. Ragauskas, C.K. Williams, B.H. Davison, G. Britovsek, J. Cairney, C.A. Eckert, W.J. Frederick Jr., J.P. Hallett, D.J. Leak, C.L. Liotta, J.R. Mielenz, R. Murphy, R. Templer, T. Tschaplinski, *Science* **311** (2006) 484-489
- [12] D.M. Alonso, J.Q. Bond, J.A. Dumesic, *Green Chem.* **12** (2010) 1493-1513

- [13] Y. Sun, J. Cheng, *Bioresource Technol.* **83** (2002) 1-11
- [14] F.S. Chakar, A.J. Ragauskas, *Ind. Crop. Prod.* **20** (2004) 131-141
- [15] G.W. Huber, S. Iborra, A. Corma, *Chem. Rev.* **106** (2006) 4044-4098
- [16] C. Crestini, M. Crucianelli, M. Orlandi, R. Saladino, *Catal. Today* **156** (2010) 8-22
- [17] D.V. Evtuguin, C. Pascoal Neto, J. Rocha, J.D. Pedrosa de Jesus, *Appl. Catal. A-Gen.* **167** (1998) 123-139
- [18] M.P. Pandey, C.S. Kim, *Chem. Eng. Technol.* **34** (2011) 29-41
- [19] H. Ben, A.J. Ragauskas, *Energ. Fuel* **25** (2011) 4662-4668
- [20] M. Kleinert, T. Barth, *Energ. Fuel* **22** (2008) 1371-1379
- [21] B. Scholze, D. Meier, *J. Anal. Appl. Pyrol.* **60** (2001) 41-54
- [22] D. C. Elliott, E.G. Baker, D. Beckman, Y. Solantausta, V. Tolénhiemo, S.B. Gevert, C. Hörnell, A. Östman, B. Kjellström, *Biomass* **22** (1990) 251-269
- [23] R.P. Nielsen, G. Olofsson, E.G. Søgaaard, *Biomass Bioenerg.* **39** (2012) 399-402
- [24] S. Bensaid, R. Conti, D. Fino, *Fuel* **94** (2012) 324-332
- [25] D. Mohan, C.U. Pittman Jr., P.H. Steel, *Energ. Fuel* **20** (2006) 848-889
- [26] A.V. Bridgwater, *Biomass Bioenerg.* **38** (2012) 68-94
- [27] P.M. Mortensen, J.-D. Grunwaldt, P.A. Jensen, K.G. Knudsen, A.D. Jensen, *Appl. Catal. A-Gen.* **407** (2011) 1-19
- [28] C. Wang, J. Pan, J. Li, Z. Yang, *Bioresource Technol.* **99** (2008) 2778-2786

- [29] H. Ben, A.J. Ragauskas, *Energ. Fuel* **25** (2011) 2322-2332
- [30] D.A. Bulushev, J.R.H. Ross, *Catal. Today* **171** (2011) 1-13
- [31] N. Joshi, A. Lawal, *Chem. Eng. Sci.* **74** (2012) 1-8
- [32] E. Furimsky, *Appl. Catal. A-Gen.* **199** (2000) 147-190
- [33] Y. Wang, Y. Fang, T. He, H. Hu, J. Wu, *Catal. Commun.* **12** (2011) 1201-1205
- [34] T.V. Choudhary, C.B. Phillips, *Appl. Catal. A-Gen.* **397** (2011) 1-12
- [35] P.T. Williams, P.A. Horne, *Biomass Bioenerg.* **7** (1994) 223-236
- [36] J.D. Adjaya, N.N. Bakhshi, *Biomass Bioenerg.* **7** (1994) 201
- [37] M.C. Samolada, W. Baldauf, I.A. Vasalos, *Fuel* **77** (1998) 1667-1675
- [38] J. Huang, W. Long, P.K. Agrawal, C.W. Jones, *J. Phys. Chem. C* **113** (2009) 16702-16710
- [39] D.C. Elliott, T.R. Hart, *Energ. Fuel* **23** (2009) 631-637
- [40] B.S. Gevert, J-E. Otterstedt, *Biomass* **13** (1987) 105-115
- [41] W. Baldauf, U. Balfanz, M. Rupp, *Biomass Bioenerg.* **7** (1994) 237-244
- [42] D.C. Elliott, T.R. Hart, G.G. Neuenschwander, L.J. Rotness, A.H. Zacher, *Environ. Prog.* **28** (2009) 441-449
- [43] D. Hong, S.J. Miller, P.K. Agrawal, C.W. Jones, *Chem. Commun.* **46** (2010) 1038-1040
- [44] T. Nimmanwudipong, R.C. Runnebaum, D.E. Block, B.C. Gates, *Energ. Fuel* **25** (2011) 3417-3427

- [45] V.N. Bui, D. Laurenti, P. Afanasiev, C. Geantet, *Appl. Catal. B-Environ.* **101** (2011) 239-245
- [46] C.A. Fisk, T. Morgan, Y. Ji, M. Crocker, C. Crofcheck, S.A. Lewis, *Appl. Catal. A-Gen.* **358** (2009) 150-156
- [47] C.L. Lee, D.F. Ollis, *J. Catal.* **87** (1984) 325-331
- [48] O.I. Senol, E.-M. Ryymin, T.-R. Viljava, A.O.I. Krause, *J. Mol. Catal A-Chem.* **277** (2007) 107-112
- [49] S. Echeandia, P.L. Arias, V.L. Barrio, B. Pawelec, J.L.G. Fierro, *Appl. Catal. B-Environ.* **101** (2010) 1-12
- [50] A. Gutierrez, R.K. Kaila, M.L. Honkela, R. Slioor, A.O.I. Krause, *Catal. Today* **147** (2009) 239-246
- [51] D.W. Green, R.H. Perry, *Perry's Chemical Engineers' Handbook* 8th ed. New York: McGraw-Hill, 2007
- [52] J.M. Prausnitz, R.N. Lichtenthaler, E.G. de Azevedo, *Molecular Thermodynamics of Fluid-Phase Equilibria* 3rd ed. New Jersey: Prentice Hall PTR, 1999
- [53] U.J. Jáuregui-Haza, E.J. Padrillo-Fontdevila, A.M. Wilhelm, H. Delmas, *Latin Am. Appl. Res.* **34** (2004) 71-74
- [54] C. Zhao, Y. Kou, A.A. Lemonidou, X. Li, J.A. Lercher, *Angew. Chem. Int. Edit.* **48** (2009) 3987-3990